

FORTIFAI: FENDING OFF RECURSIVE TRAINING INDUCED FAILURE FOR AI MODELS

Soheil Zibakhsh Shabgahi^{†1} Pedram Aghazadeh^{†1} Azalia Mirhoseini² Farinaz Koushanfar¹

¹ University of California San Diego

² Stanford University

{szibakhshshabgahi, paghazadeh, farinaz}@ucsd.edu azalia@stanford.edu

ABSTRACT

The increasing reliance on generative AI models is rapidly increasing the volume of synthetic data, with some projections suggesting that most available new data for training could be machine-generated by 2030 Gartner, Inc. (2022). This shift to a mainly synthetic content presents a critical challenge: repeated training in synthetic data leads to a phenomenon known as model collapse, where model performance degrades over generations of training, eventually rendering the models ineffective. While the causes of model collapse are increasingly understood, effective mitigation strategies remain scarce. We address this challenge by leveraging a key insight: auto-regressive models tend to generate text sequences to which they assign high confidence (i.e., high log-likelihood). Based on this observation, we introduce the Truncated-Cross-Entropy (TCE) loss function. TCE mitigates collapse by selectively ignoring high-confidence tokens during training, effectively filtering out likely machine-generated artifacts from the learning process. Our experiments demonstrate that models trained with TCE not only learn effectively but also exhibit significantly increased resilience, tolerating over 2.3 \times more synthetic data before the onset of collapse. In addition, we provide an open-source benchmark for collapse dynamics in mixed-data settings. Our results demonstrate that confidence-aware training objectives can substantially delay collapse onset, offering a practical and generalizable tool for model robustness under synthetic-data exposure.

1 INTRODUCTION

Generative models have become the foundation for modern AI applications in several modalities, including text, image, code, and audio. Large Language Models (LLMs) such as ChatGPT (OpenAI et al., 2024), LLaMA (Grattafiori et al., 2024) and Gemma (Team et al., 2025), as well as image generators DALL-E (Ramesh et al., 2021) and Imagen (Saharia et al., 2022), all rely on large datasets scraped from the Web. As these models are continuously updated to reflect recent knowledge and linguistic patterns, the need for ever larger and frequently refreshed training corpora has grown substantially. However, this demand is colliding with a shift in the data landscape: synthetic content is increasingly populating the Internet, contaminating the very datasets used for model training.

This shift raises fundamental concerns. Generative models trained on outputs from earlier generations can degrade over time, a phenomenon known as *model collapse* (Shumailov et al., 2024a;b; Dohmatob et al., 2024b). Even moderate levels of synthetic data (as little as 1%) have been shown to cause collapse, and scaling the model or the size of the dataset fails to reliably prevent it (Dohmatob et al., 2024a). Importantly, this is not a hypothetical scenario: recent analysis of Alemohammad et al. (2023) on the LAION-5B dataset, a cornerstone for many generative models, revealed measurable contamination from synthetic sources.¹ As synthetic data becomes dominant, safeguarding generative model stability becomes an urgent challenge.

[†]Equal contribution.

¹Following prior works (Shumailov et al., 2024a;b), we use the term *contamination* or *poisoning* to describe the recursive use of synthetic data in training, which leads to degradation in performance over generations.

Several approaches have been explored to mitigate model collapse. Some studies combine synthetic and real data to slow degradation (Gerstgrasser et al., 2024); others rely on post hoc supervision, such as SIMS (Alemohammad et al., 2024), using labeled synthetic data as negative signal to improve generations or explore decoding strategies (Drayson et al., 2025). In practice, however, distinguishing real from synthetic data remains a major challenge. Watermarking methods (Zhang & Koushanfar, 2024; Kirchenbauer et al., 2024) have been proposed to help identify model-generated content, but they are not widely adopted. Moreover, recent critiques (Schaeffer et al., 2025) highlight that many prior studies simulate collapse in unrealistic settings, such as using purely synthetic training data, limiting the applicability of their conclusions. Despite growing interest in this issue, the role of the loss function, central to how models learn, has received little attention in the context of model collapse.

In this work, we present ForTIFAI, showing that model collapse can be mitigated through principled modifications to training loss. We argue that generative models tend to be overconfident in their synthetic predictions (as depicted in Figure 1), causing feedback loops that degrade performance. This issue is further amplified by approximation errors and finite sampling effects during training, which cause models to concentrate probability mass on a shrinking subset of the true data distribution over generations (Shumailov et al., 2024b; Dohmatob et al., 2024b). To address this challenge, we introduce Truncated Cross-Entropy (TCE), a loss function that formalizes the intuition of ignoring what the model already “knows” too well. TCE operates by setting the loss to zero for any token whose predicted probability exceeds a predefined threshold. This prevents the model from overfitting to its own high-conviction and often low-diversity outputs. As a minimal extension of the standard Cross-Entropy (CE) objective, TCE is model-agnostic, computationally efficient, and easy to implement, making it a practical solution for real-world deployment.

In brief, the contributions of ForTIFAI are as follows:

- We establish that a model’s confidence, measured by sequence probability, serves as a strong signal for identifying its own generated text within mixed datasets.
- We introduce Truncated Cross Entropy (TCE), a confidence-aware loss function that leverages this signal to mitigate model collapse, enabling models to tolerate more than $2.3\times$ greater proportions of synthetic data without degradation.
- We propose a comprehensive evaluation framework for model collapse that reflects realistic conditions, including the continual accumulation of new data and the need to measure both retained and newly acquired knowledge.

2 METHOD

2.1 PROBLEM DEFINITION

Model Collapse is the gradual degradation that occurs when a model’s own outputs pollute the training data of its successors. Each new model then learns from these possibly flawed examples, causing a drift from the true data distribution (Shumailov et al., 2024a).

The fundamental cause of collapse is the discrepancy between the true data distribution, P_{data} , and the model’s learned approximation of it, P_θ . Because any realizable model has finite capacity and is trained on finite data, its outputs will contain statistical artifacts not present in the true distribution. Compounding this issue, the decoding process itself introduces a further distributional shift. Common decoding algorithms (e.g., greedy search, beam search) are designed to favor high-probability sequences rather than sampling purely from the model’s learned distribution. This bias means that even if a model were a perfect representation of the data ($P_\theta = P_{data}$), the generated text would over-represent the modes of the distribution.

When these skewed outputs are used to train a successor model, the imperfections are learned and amplified. This iterative process leads to a progressive distributional drift, causing a catastrophic loss of information, particularly in the tails of the distribution, ultimately making the model unusable.

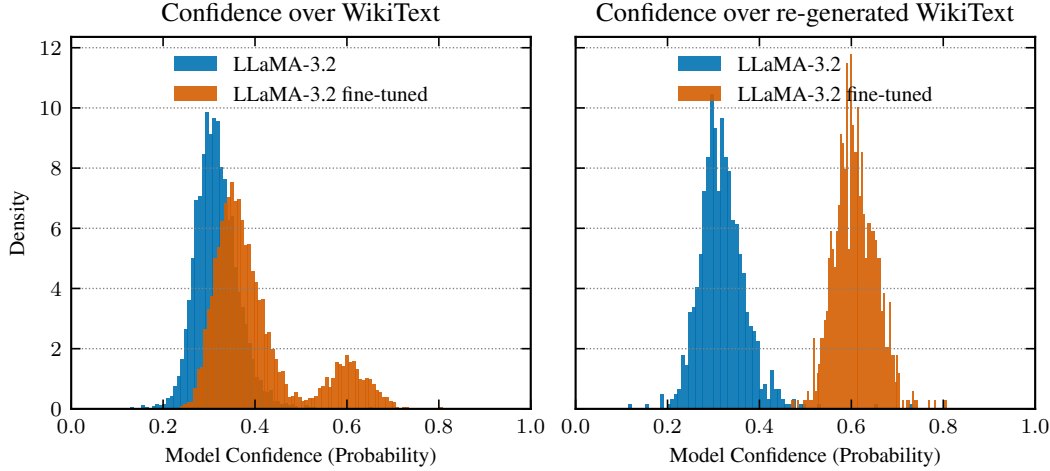


Figure 1: A model exhibits significantly higher confidence in its own generated data compared to unseen data. The histograms show token probabilities from a base LLaMA-3.2-1B model (blue) and a fine-tuned version (orange). When evaluating its own synthetic generations (right column), the fine-tuned model shows a clear shift toward higher confidence compared to its evaluation on unseen data (left column). In contrast, the base model’s confidence distribution remains consistent across both datasets, identifying elevated confidence as a sign of self-generated text.

2.2 KEY OBSERVATION

Figure 1 illustrates a consistent gap in model confidence between self-generated samples and unseen data. We exploit this difference as a signal to identify and remove the effect of synthetic samples during training. This gap is a side effect of the approximation error and the greedy sampling performed for generating text (Drayson et al., 2025).

2.3 TRUNCATED CROSS ENTROPY (TCE)

Building on the findings from Section 2.2, we introduce a novel loss function, Truncated Cross Entropy (TCE). In TCE, confident predictions are explicitly masked to remove their influence on training. By selectively masking overly confident predictions, TCE forces the model to learn from less-certain datapoints, thereby preserving distribution tails compared to CE. We formulate TCE as:

$$TCE(p_t) = \chi_\gamma(p_t) \times CE(p_t)$$

$$\chi_\gamma(p_t) = \begin{cases} 1 & \text{if } p_t \leq \gamma \\ 0 & \text{if } p_t > \gamma \end{cases}$$

Here, p_t is the probability of the correct class, $\chi_\gamma(\cdot)$ is an indicator function, $CE(\cdot)$ is the cross-entropy loss, and $\gamma \in [0, 1]$ is the confidence threshold. Setting γ close to 1 recovers standard CE loss, while smaller values selectively suppress high-confidence predictions. In Appendix A we examine Focal Loss as another alternative confidence-aware loss function with similar properties.

2.4 MATHEMATICAL INSIGHT

The growing reliance on synthetic data in generative model training pipelines has given rise to a self-consuming feedback loop wherein models are recursively trained on their own outputs.

In a fully synthetic training loop, where each model G_t is trained solely on samples from G_{t-1} , Alemohammad et al. (2023) prove that the model’s estimated covariance σ_t collapses almost surely:

$$\mathbb{E}[\sigma_t | \sigma_{t-1}] = \lambda \sigma_{t-1}, \quad \text{with } \lambda \leq 1, \quad \Rightarrow \quad \sigma_t \xrightarrow{a.s.} 0. \quad (1)$$

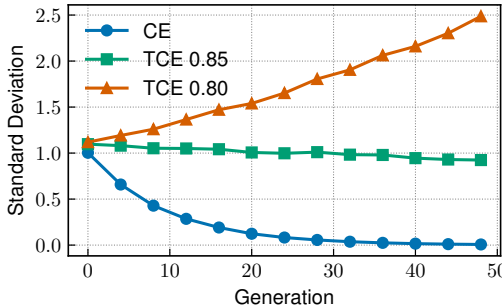


Figure 2: Effect of TCE on a one-dimensional Gaussian estimator under a fully synthetic training loop. In each generation, 10,000 samples are generated with sampling bias $\gamma = 0.9$. Standard estimation with Cross Entropy (CE) leads to rapid variance collapse. By contrast, TCE with a well-chosen threshold ($\gamma = 0.85$) delays collapse substantially. Conversely, if the threshold is set too small ($\gamma = 0.80$), the variance may diverge.

where λ represents sampling bias, contracting the variance at each iteration, leading to rapid loss of sample diversity, as illustrated in Figure 2. This decrease in variance is empirically observed across models such as DDPMs (Ho et al., 2020) and StyleGAN-2 (Karras et al., 2020).

To build intuition on how to counteract this collapse, we analyze a one-dimensional Gaussian model where data is drawn from $X_t \sim \mathcal{N}(0, \sigma_t^2)$. Our strategy is to modify the training objective to focus on low-probability samples. In our Gaussian case, this is equivalent to training only on samples from the tails of the distribution, i.e., where $|X_t| \geq a\sigma_t$ for a chosen threshold $a > 0$.

The conditional variance of this truncated distribution is given by:

$$\text{Var}(X_t \mid |X_t| \geq a\sigma_t) = \eta(a) \cdot \sigma_t^2, \quad (2)$$

where $\eta(a)$ is a variance amplification factor. Using known properties of the truncated normal distribution, this factor is calculated as:

$$\eta(a) = 1 + \frac{a\phi(a)}{1 - \Phi(a)} \quad (3)$$

where $\phi(\cdot)$ and $\Phi(\cdot)$ are the standard normal PDF and CDF, respectively. Crucially, $\eta(a) > 1$ for all $a > 0$.

By incorporating this variance amplification into the self-consuming loop, the recurrence for the variance becomes:

$$\mathbb{E}[\sigma_{t+1}^2] = \lambda \cdot \eta(a) \cdot \mathbb{E}[\sigma_t^2]. \quad (4)$$

The collapse can now be slowed by choosing a threshold a such that the combined factor $\lambda \cdot \eta(a) \approx 1$, stabilizing the training process by preserving sample diversity.

We argue that overconfident predictions on common tokens can dominate the training signal, ultimately causing the model to under-represent less frequent but meaningful patterns. If not addressed, this effect progressively narrows the model's output distribution, highlighting the importance of suppressing overconfident learning.

By generalizing this principle from a Gaussian model to general generative models, we propose augmenting loss functions to address this issue. **Truncated Cross Entropy (TCE)** explicitly masks the contribution of high-confidence predictions. This shifts the training signal toward low-confidence, often underrepresented tokens, mitigating the tail-vanishing effect and reducing the recursive amplification of statistical errors highlighted above.

3 MODEL COLLAPSE EVALUATION FRAMEWORK

To realistically assess the impact of *Model Collapse*, we adopt an experimental framework inspired by Gerstgrasser et al. (2024). Initially, web data was predominantly human-generated and often

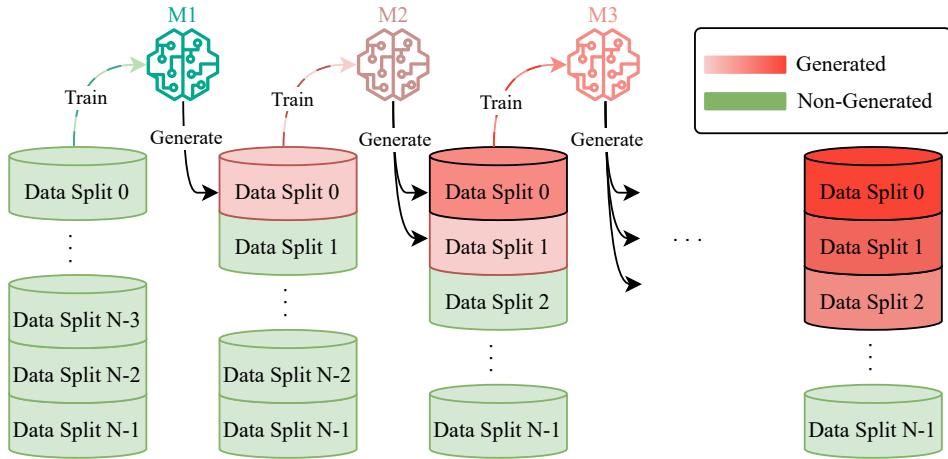


Figure 3: Our experimental setup simulates model collapse, illustrating the transition from predominantly human-generated content to mostly synthetic datasets. M_i denotes the i -th generation of recursively trained models. The clean data is initially split into N equally sized splits. At each generation, the entire dataset from the previous iteration is regenerated and used as training data for the next iteration. One split of clean data is added to this training dataset to simulate the accumulation of non-generated data into the training set. The red color for each data split indicates the contamination from recursively training on the self-generated data, resulting in lower quality (darker red color)

curated for quality. Over time, however, machine-generated content, often indistinguishable from human-written text, has increasingly supplemented online data. Our framework simulates a realistic model collapse process by progressively adding synthetic data to the training set. We evaluate the methods on math, reasoning, and knowledge recall benchmark performance. Moreover, we analyze the number of synthetic training iterations it takes for the model to lose performance below a certain threshold, which we call the time to failure.

As illustrated in Figure 3, the experiment proceeds in multiple stages. At each stage, the dataset simulates a large-scale pretraining corpus, composed of both authentic and self-generated data. At every step, we regenerate the previous stage’s dataset using the latest model and concatenate the dataset with a fixed amount of new human-written text. This new dataset is then used to further train the model, as detailed further in Algorithm 1.

This setup also follows the conditions mentioned in Schaeffer et al. (2025):

1. **Increasing Pre-training Data:** Unlike previous studies with fixed dataset sizes, our setup continuously increases the pre-training data at each generation. This growth mirrors real-world trends among state-of-the-art models; for example, LLaMA 1, 2, and 3 were trained on 1.4, 2, and 15 trillion tokens, respectively. Although dataset growth has eventual limits, these bounds remain extremely high (approximately one quadrillion tokens) Villalobos et al. (2024), far exceeding current dataset sizes.
2. **Synthetic Data Accumulation Alongside Real Data:** Another distinctive feature of our framework is its simultaneous training on both real and synthetic data. Unlike previous work, we do not discount the effect of real unseen data on model collapse. We argue that the real unseen data is the main reason behind training the new generation of models in the first place.
3. **Decreasing Proportion of Real Data:** A primary concern highlighted in recent literature is the accelerating generation rate of synthetic data and its impact on future generative models. Our experimental setup realistically emulates this crucial aspect (e.g. in our setup with 6 stages, we have 100%, 50%, 33%, 25%, 20%, and 15% real data at each stage, respectively).

Algorithm 1 Recursive data generation with an LLM

```

1: Inputs:
2:    $N \geq 2$ 
3:    $N + 1$  splits of authentic dataset  $D_0^{(0)}, \dots, D_N^{(0)}$ , each of equal size
       $\triangleright D_i^{(j)}$  is the  $j$ -th generation of the  $i$ -th split.
4:    $N + 1$  evaluation sets  $Eval_0, \dots, Eval_N$ , each of equal size
       $\triangleright Eval_i$  is based on the content of  $D_i^{(0)}$ .
5:    $M_0 \Leftarrow$  Pretrained model
6:   for  $i = 0 \rightarrow N$  do
7:     Train  $M_i$  on  $[D_0^{(i)}, D_1^{(i-1)}, \dots, D_i^{(0)}]$ 
8:     for  $k = 0 \rightarrow i$  do
9:        $D_k^{(i+1-k)} \Leftarrow M_i(D_k^{(i-k)})$ 
10:      Evaluate  $M_i$  on  $Eval_k$ 
11:    end for
12:     $M_{i+1} \Leftarrow M_i$ 
13:  end for

```

4 RESULTS

To demonstrate the effectiveness of Truncated Cross Entropy, we evaluate it across three settings: Transformers, Variational Autoencoders, and Gaussian Mixture Models. For Transformers, we focus on language modeling, testing LLaMA 3 Grattafiori et al. (2024) and Gemma 3 Team et al. (2025) on benchmarks for mathematical reasoning, logical inference, and factual recall. For image generation, we use Variational Autoencoders, and for mixture modeling, we evaluate standard GMMs. Across all experiments, our loss function mitigates model collapse without degrading overall training performance.

4.1 EXPERIMENT DETAILS

We apply the recursive training setup illustrated in Figure 3 on two datasets: Wikitext-2-raw-v1 Merity et al. (2016) and a newly curated dataset called *Imagination of Web*.

4.1.1 DATASETS

Wikitext-2-raw-v1 is a language modeling dataset derived from high-quality Wikipedia articles. Unlike its tokenized counterpart, it preserves raw formatting—including punctuation, casing, and whitespace—making it well-suited for evaluating a model’s ability to handle long-range dependencies and natural language structure.

The second dataset, *Imagination of Web*, is a composite dataset constructed from subsets of Wiki-text, HellaSwag Zellers et al. (2019), and GSM8k Cobbe et al. (2021). It is designed to test the generalization of our loss functions across multiple tasks, such as commonsense, math, and factual recall.

4.1.2 FRAMEWORK PARAMETERS

We used the framework described in Section 3 to simulate a progressive model collapse scenario.

For our experiments, we set the number of stages to $N = 6$. We found that model collapse was not reliably observable for fewer than six stages, while increasing N beyond six introduced significant computational overhead with diminishing returns under our resource constraints. For simplicity, we used a fixed amount of data at each stage from the original dataset.

4.1.3 HYPERPARAMETERS

For both LLaMA and Gemma model families, we tuned and used the best-performing hyperparameters. All models were fine-tuned using a learning rate of 2×10^{-5} , with a batch size of 64. The training was conducted over 10 epochs per stage with the best performing checkpoints saved.

4.2 EVALUATION BENCHMARKS

To comprehensively assess the impact of our loss functions on model performance and resilience to model collapse, we perform evaluations on a mix of standard and custom benchmarks. These benchmarks test various capabilities including factual recall, linguistic coherence, commonsense, and mathematical reasoning. In addition to widely used benchmarks like BLiMP, Hellaswag, and GSM8K, we introduce a new question-answering benchmark—*Knowledge Retention test* (KR-test) to measure how well models retain training-set facts.

4.2.1 KNOWLEDGE RETENTION TEST

Validation perplexity is a common metric for evaluating LLMs, but it primarily reflects predictive fluency; how well a model guesses the next token in unseen text. While useful for assessing grammar and style, it does not quantify factual knowledge retention. Moreover, low perplexity does not guarantee meaningful or human-like output, as humans do not always select the most likely next word.

To address this gap, we introduce the *Knowledge Retention Test* (KR-test), which measures factual *retention* from the training data rather than general fluency.

Given a body of training text, we divide it into complete paragraphs and generate five questions per paragraph. Each question consists of a context, a true continuation, and a false continuation.

We compute the log probability of the model for two sequences:

- *Context + Factually correct completion*
- *Context + Factually incorrect completion*

When the log probability is higher for the true continuation, the question is considered correctly answered. The KR-test score is the model’s total accuracy over all the questions.

A high KR-test score indicates that the model has internalized the factual content of the paragraph. This benchmark specifically tests factual retention from the training data. More details on KR-test can be found in Appendix B. In Fig. 4 superiority of TCE compared to the baseline is shown after six iterations in correctly answering questions about Wikitext.

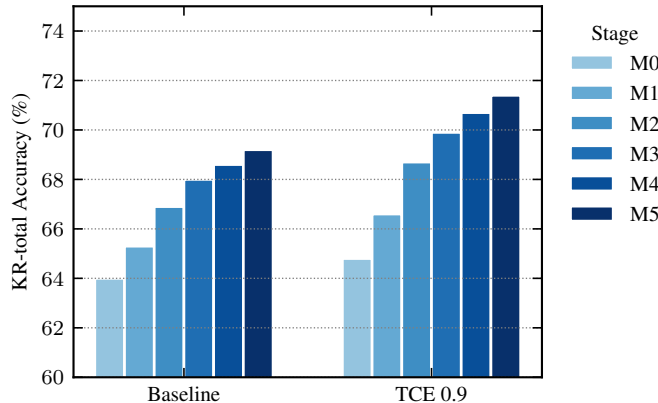


Figure 4: Total knowledge retention (KR-total) accuracy with LLaMA-3.2-1B model trained on Wikitext. TCE retains learning capability and even exceed the baseline throughout different stages.

4.2.2 MATH, REASONING, AND COHERENCE

In addition to factual retention, we evaluate model’s performance across three reasoning and language understanding benchmarks. These evaluations assess whether our loss functions preserve or enhance generalization and linguistic structure, both of which are vulnerable under recursive training regimes.

To evaluate the impact of model collapse on reasoning and linguistic capability, we use three standard benchmarks: **GSM8K** Cobbe et al. (2021), **Hellaswag** Zellers et al. (2019), and **BLiMP** Warstadt et al. (2023).

- **GSM8K** measures mathematical reasoning by testing the model’s ability to solve grade-school level word problems. Success on this benchmark reflects the model’s ability to perform multi-step arithmetic reasoning.
- **Hellaswag** evaluates commonsense reasoning through multiple-choice sentence completion tasks. It requires the model to infer plausible continuations based on everyday scenarios.
- **BLiMP** tests grammatical coherence and syntactic structure. It consists of minimal pairs where the model must choose the grammatically correct option. High performance indicates strong control over syntax and language structure.

Together, these benchmarks assess the model’s ability to generalize, reason, and maintain coherence under different forms of linguistic stress. For **GSM8K** and **Hellaswag**, we use the Language Model Evaluation Harness Gao et al. (2024) to ensure consistent evaluation across models.

4.3 WIKITEXT DATASET

To assess performance under idealized, non-collapsing conditions, we also evaluate models trained exclusively on original, non-synthetic data. The results, shown in Table 1, confirm that **FL** and **TCE 0.9** maintain strong performance in streamline training settings.

Table 2 presents the results after 5 stages of synthetic data accumulation as discussed in Section 3. The evaluation spans across the full benchmark suite, excluding **GSM**, since the **Wikitext** training dataset does not include any math or reasoning. On average, **FL** outperforms **CE** by 3.8% for **LLaMA-3.2-1B** and 1.3% for **Gemma-3-1b-pt**. Overall, **TCE 0.9** outperforms **CE**, especially in preserving factual knowledge.

Table 1: Comparison of **LLaMA** and **Gemma** models on **M0** (clean and non-generated data) across **Blimp**, **Hellaswag**, **GSM8k**, and **KR-test** on *Wikitext dataset*. For **LLaMA** and **Gemma**, **TCE** outperforms baseline (**CE**) when trained on real non-generated data. The highest value per block is **bolded**.

| Model | Method | Blimp | Hellaswag | KR-test | Average |
|-------|----------|--------------|--------------|--------------|--------------|
| LLaMA | Baseline | 75.1% | 58.5% | 64.0% | 65.86% |
| | TCE 0.9 | 76.8% | 61.8% | 64.8% | 67.8% |
| Gemma | Baseline | 71.2% | 63.9% | 67.7% | 67.6% |
| | TCE 0.9 | 73.9% | 64.6% | 68.2% | 68.9% |

Table 2: Comparison of **M5** benchmark results across **LLaMA** and **Gemma** models for Baseline, and **TCE 0.9** methods on *Wikitext dataset*. The highest value per block is **bolded**.

| Model | Method | Blimp | Hellaswag | KR-test | Average |
|-------|----------|--------------|--------------|--------------|---------------|
| LLaMA | Baseline | 63.3% | 45.7% | 69.2% | 59.4% |
| | TCE 0.9 | 63.6% | 48.4% | 71.4% | 61.13% |
| Gemma | Baseline | 61.2% | 52.4% | 68.1% | 60.56% |
| | TCE 0.9 | 61.8% | 53% | 69.7% | 61.5% |

Performance of both models when experiment is conducted on **Wikitext** dataset is shown in Fig. 5 where **TCE** consistently outperforms **CE** during different stages of the experiment.

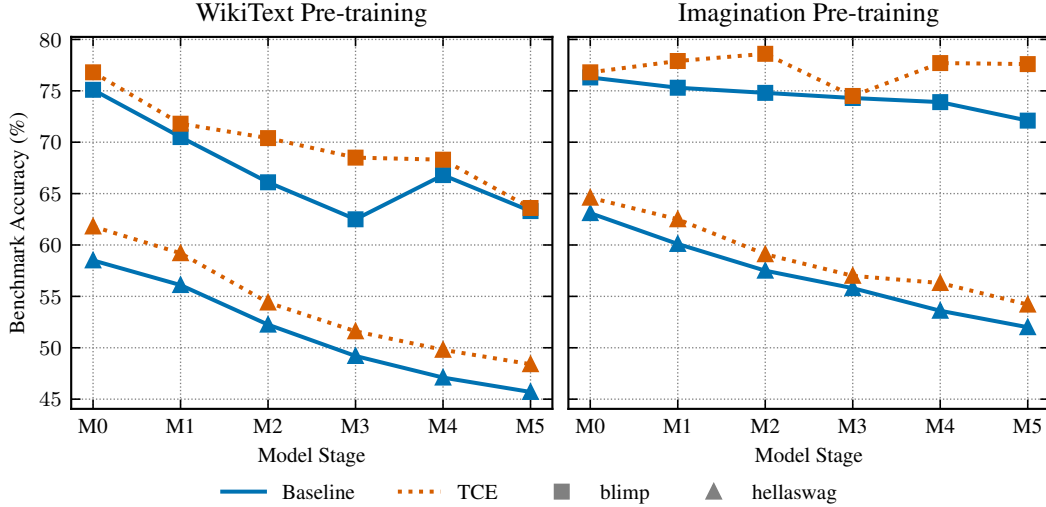


Figure 5: Our proposed solution outperforms baselines (CE) across all benchmarks consistently when experiment is done on both datasets. Figures (a) and (b) show the results of LLaMA-3.2-1B across different benchmarks.

4.4 IMAGINATION-OF-WEB DATASET

To evaluate in a setting closer to real-world pre-training, we adopt the *Imagination-of-Web* (IoW) corpus—a composite of factual prose (Wikitext), commonsense reasoning (HellaSwag), and mathematical problem solving (GSM8K).

Table 3 reports clean-data results. Here, TCE surpasses CE by 1.8% on LLaMA-3.2-1B and 1.3% on Gemma-3-1b-pt, confirming the strong learning capability of performance under non-collapsing conditions.

Table 3: Comparison of LLaMA and Gemma models on M0 (clean and non-generated data) across Blimp, Hellaswag, GSM8k, and KR-total on *Imagination dataset*. The highest value per block is **bolded**, and the second highest is underlined.

| Model | Method | Blimp | Hellaswag | GSM8k | KR-total | Average |
|-------|------------------------|--------------|--------------|-------------|--------------|---------------|
| LLaMA | Baseline | 76.3% | 63.1% | 8.1% | 63.6% | 58.78% |
| | Focal ($\gamma = 2$) | 79.6% | 65.2% | 9.5% | 64.8% | 60.62% |
| | TCE 0.9 | <u>76.8%</u> | <u>64.6%</u> | <u>9.1%</u> | <u>64.8%</u> | <u>59.52%</u> |
| Gemma | Baseline | 73.1% | 65% | 6.2% | 64.1% | 52.1% |
| | Focal ($\gamma = 2$) | 77.2% | 65.7% | 4.5% | 64.2% | 52.9% |
| | TCE 0.9 | <u>76%</u> | 65% | <u>5.2%</u> | 64% | <u>52.55%</u> |

Table 4 shows outcomes after five rounds of synthetic data accumulation. TCE 0.9 outperforms CE by 3.6% on LLaMA-3.2-1B and 0.4% on Gemma-3-1b-pt. As on Wikitext, TCE preserves factual and reasoning accuracy, reinforcing its robustness against model collapse in heterogeneous training scenarios.

Performance of both models when experiment is conducted on Imagination dataset is shown in Fig. 5, where TCE consistently outperform CE during different stages of the experiment.

4.5 TIME TO FAILURE

We define *time to failure* as the number of re-training tokens it takes a model in the context of this framework to degrade significantly compared to the initial model. Specifically, we analyze the performance of the model on the first partition of the dataset, which is re-generated at each

Table 4: Comparison of M5 benchmark results across LLaMA and Gemma models for Baseline and TCE 0.9 method on *Imagination dataset*. The highest value per block is **bolded**.

| Model | Method | Blimp | Hellaswag | GSM8k | KR-total | Average |
|-------|----------|--------------|--------------|-------------|--------------|---------------|
| LLaMA | Baseline | 72.1% | 52.0% | 5.9% | 68.7% | 52.94% |
| | TCE 0.9 | 77.6% | 54.2% | 6.2% | 71.0% | 55.52% |
| Gemma | Baseline | 71% | 53.4% | 3.9% | 71.6% | 49.97% |
| | TCE 0.9 | 71.7% | 53.1% | 4.2% | 74.1% | 50.77% |

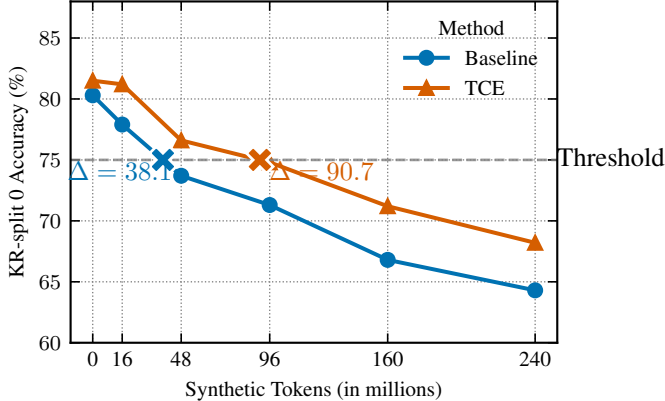


Figure 6: Our proposed loss functions effectively mitigate model collapse in a fully synthetic subset of the dataset. The figure above corresponds to LLaMA-3.2-1B’s accuracies on answering questions related to the dataset they were trained on. Red dotted lines provided for better comparison of time to failure. The number of stages until failure is shown as Δ .

stage. Moreover, since the KR-test on average has a baseline of 50% and a maximum of 100% is achievable, we define failure as performance dropping below 75%, which is exactly half the maximum gain one can expect from training the model. As illustrated in Figure 6, Cross Entropy collapses (reaches 75% accuracy) between the first and the second generation and both TCE reaches this point after three stages of self-consuming generation, increasing the time to failure by $2.3\times$.

4.6 KL DIVERGENCE

To quantify distributional drift across generations, we measured the Kullback–Leibler (KL) divergence between the token distributions of synthetic datasets and the original WikiText-2 corpus. Each dataset is tokenized with the model’s tokenizer, and normalized token frequencies are used to compute the KL divergence between the original and synthetic distributions.

Figure 7 shows that models trained with TCE maintain a substantially lower KL divergence than those trained with Cross Entropy, indicating better preservation of the original data distribution.

5 CONCLUSION

We have demonstrated that a confidence-aware loss function, Truncated Cross-Entropy (TCE), provides a simple and powerful defense against model collapse. Grounded in a mathematical framework linking overconfidence to distributional drift, TCE extends a model’s operational lifetime by over $1.7\times$ compared to standard cross-entropy. Our benchmarks confirm that this approach not only delays collapse but also improves knowledge retention and generalization in environments with accumulating synthetic data, as validated by slower KL divergence growth.

Crucially, the principle of filtering overconfident outputs is not domain-specific. We verified its efficacy in diverse generative systems, including Gaussian Mixture Models and Variational Autoen-

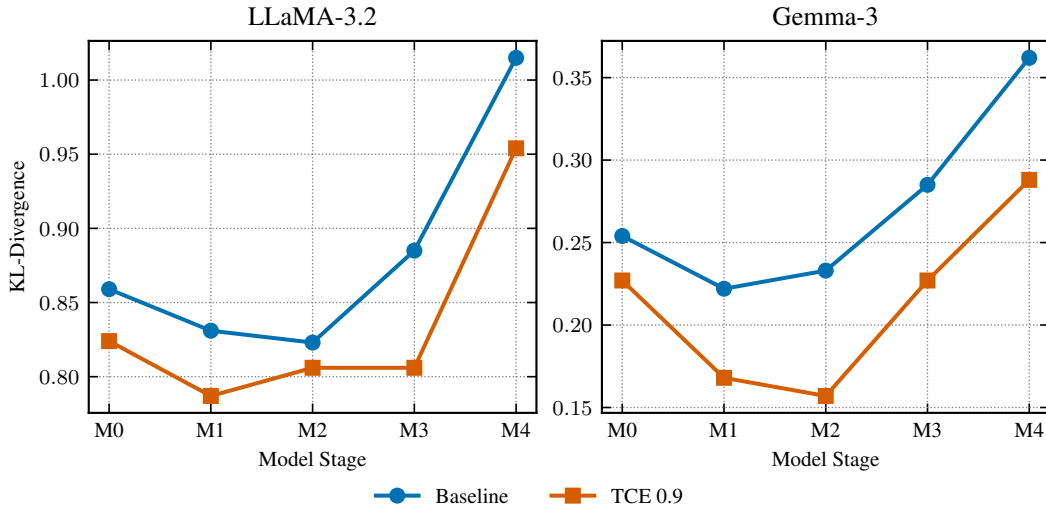


Figure 7: To quantify collapse dynamics, we measured the Kullback-Leibler (KL) divergence between the distribution of model-generated outputs and the original training data distribution over successive generations of the WikiText dataset. Models trained with Cross Entropy showed rapidly increasing KL divergence, indicating distributional drift and loss of diversity. In contrast TCE and significantly slowed the divergence growth, effectively preserving distributional similarity across generations.

coders (Appendices F, G). As the line between human and machine-generated data continues to blur, such robust, low-overhead training methods will be essential for building stable and trustworthy AI.

5.1 FUTURE DIRECTIONS

We approached model collapse from a training perspective and proposed a class of loss functions that mitigate collapse effectively without sacrificing performance. By reweighting token probabilities to favor underrepresented or underestimated outputs, these losses retain the simplicity of cross-entropy while offering greater resilience during recursive training.

Looking ahead, several research avenues merit further exploration:

- **Broader Model Classes:** Model collapse has been extensively studied in image generation domains. It remains an open question whether similar loss-based strategies can be adapted to diffusion models (Ho et al., 2020) and generative adversarial networks (GANs) (Goodfellow et al., 2014), where diversity collapse is also a central concern.
- **Heterogeneous Model Ecosystems:** Our setup assumes a single model trained recursively across generations. However, real-world content generation is inherently multi-agent and heterogeneous, involving a mixture of open and closed-source models. Extending our analysis to simulate ecosystems of interacting generative models could provide deeper insights into how synthetic content evolves when shaped by a plurality of architectures and training paradigms.
- **Collapse-Aware Generation:** While our approach targets the training process, model collapse can also be addressed during the generation phase. Combining our training-side solution with decoding-aware techniques such as Drayson et al. (2025) may yield complementary benefits, improving the quality and diversity of generated data further.

REFERENCES

Sina Alemohammad, Josue Casco-Rodriguez, Lorenzo Luzi, Ahmed Imtiaz Humayun, Hossein Babaei, Daniel LeJeune, Ali Siahkoohi, and Richard G. Baraniuk. Self-consuming generative models go mad, 2023. URL <https://arxiv.org/abs/2307.01850>.

Sina Alemohammad, Ahmed Imtiaz Humayun, Shruti Agarwal, John Collomosse, and Richard Baraniuk. Self-improving diffusion models with synthetic data, 2024. URL <https://arxiv.org/abs/2408.16333>.

Karl Cobbe, Vineet Kosaraju, Mohammad Bavarian, Mark Chen, Heewoo Jun, Lukasz Kaiser, Matthias Plappert, Jerry Tworek, Jacob Hilton, Reiichiro Nakano, Christopher Hesse, and John Schulman. Training verifiers to solve math word problems, 2021. URL <https://arxiv.org/abs/2110.14168>.

Li Deng. The mnist database of handwritten digit images for machine learning research [best of the web]. *IEEE Signal Processing Magazine*, 29(6):141–142, 2012. doi: 10.1109/MSP.2012.2211477.

Elvis Dohmatob, Yunzhen Feng, Arjun Subramonian, and Julia Kempe. Strong model collapse, 2024a. URL <https://arxiv.org/abs/2410.04840>.

Elvis Dohmatob, Yunzhen Feng, Pu Yang, Francois Charton, and Julia Kempe. A tale of tails: Model collapse as a change of scaling laws, 2024b. URL <https://arxiv.org/abs/2402.07043>.

George Drayson, Emine Yilmaz, and Vasileios Lampos. Machine-generated text detection prevents language model collapse, 2025. URL <https://arxiv.org/abs/2502.15654>.

Leo Gao, Jonathan Tow, Baber Abbasi, Stella Biderman, Sid Black, Anthony DiPofi, Charles Foster, Laurence Golding, Jeffrey Hsu, Alain Le Noac'h, Haonan Li, Kyle McDonell, Niklas Muenninghoff, Chris Ociepa, Jason Phang, Laria Reynolds, Hailey Schoelkopf, Aviya Skowron, Lintang Sutawika, Eric Tang, Anish Thite, Ben Wang, Kevin Wang, and Andy Zou. The language model evaluation harness, 07 2024. URL <https://zenodo.org/records/12608602>.

Gartner, Inc. Is synthetic data the future of ai?, June 2022. URL <https://www.gartner.com/en/newsroom/press-releases/2022-06-22-is-synthetic-data-the-future-of-ai>. Accessed: 2025-05-29.

Matthias Gerstgrasser, Rylan Schaeffer, Apratim Dey, Rafael Rafailov, Henry Sleight, John Hughes, Tomasz Korbak, Rajashree Agrawal, Dhruv Pai, Andrey Gromov, Daniel A. Roberts, Diyi Yang, David L. Donoho, and Sanmi Koyejo. Is model collapse inevitable? breaking the curse of recursion by accumulating real and synthetic data, 2024. URL <https://arxiv.org/abs/2404.01413>.

Ian J. Goodfellow, Jean Pouget-Abadie, Mehdi Mirza, Bing Xu, David Warde-Farley, Sherjil Ozair, Aaron Courville, and Yoshua Bengio. Generative adversarial networks, 2014. URL <https://arxiv.org/abs/1406.2661>.

Aaron Grattafiori, Abhimanyu Dubey, Abhinav Jauhri, Abhinav Pandey, Abhishek Kadian, Ahmad Al-Dahle, Aiesha Letman, Akhil Mathur, Alan Schelten, Alex Vaughan, Amy Yang, Angela Fan, Anirudh Goyal, Anthony Hartshorn, Aobo Yang, Archi Mitra, Archie Sravankumar, Artem Korenev, Arthur Hinsvark, Arun Rao, Aston Zhang, Aurelien Rodriguez, Austen Gregerson, Ava Spataru, Baptiste Roziere, Bethany Biron, Binh Tang, Bobbie Chern, Charlotte Caucheteux, Chaya Nayak, Chloe Bi, Chris Marra, Chris McConnell, Christian Keller, Christophe Touret, Chunyang Wu, Corinne Wong, Cristian Canton Ferrer, Cyrus Nikolaidis, Damien Allonsius, Daniel Song, Danielle Pintz, Danny Livshits, Danny Wyatt, David Esiobu, Dhruv Choudhary, Dhruv Mahajan, Diego Garcia-Olano, Diego Perino, Dieuwke Hupkes, Egor Lakomkin, Ehab AlBadawy, Elina Lobanova, Emily Dinan, Eric Michael Smith, Filip Radenovic, Francisco Guzmán, Frank Zhang, Gabriel Synnaeve, Gabrielle Lee, Georgia Lewis Anderson, Govind That-tai, Graeme Nail, Gregoire Mialon, Guan Pang, Guillem Cucurell, Hailey Nguyen, Hannah Korevaar, Hu Xu, Hugo Touvron, Iliyan Zarov, Imanol Arrieta Ibarra, Isabel Kloumann, Ishan Misra, Ivan Evtimov, Jack Zhang, Jade Copet, Jaewon Lee, Jan Geffert, Jana Vranes, Jason Park, Jay Mihadeokar, Jeet Shah, Jelmer van der Linde, Jennifer Billock, Jenny Hong, Janya Lee, Jeremy Fu, Jianfeng Chi, Jianyu Huang, Jiawen Liu, Jie Wang, Jiecao Yu, Joanna Bitton, Joe Spisak, Jong-soo Park, Joseph Rocca, Joshua Johnstun, Joshua Saxe, Junteng Jia, Kalyan Vasudevan Alwala, Karthik Prasad, Kartikeya Upasani, Kate Plawiak, Ke Li, Kenneth Heafield, Kevin Stone, Khalid

El-Arini, Krithika Iyer, Kshitiz Malik, Kuenley Chiu, Kunal Bhalla, Kushal Lakhota, Lauren Rantala-Yearly, Laurens van der Maaten, Lawrence Chen, Liang Tan, Liz Jenkins, Louis Martin, Lovish Madaan, Lubo Malo, Lukas Blecher, Lukas Landzaat, Luke de Oliveira, Madeline Muzzi, Mahesh Pasupuleti, Mannat Singh, Manohar Paluri, Marcin Kardas, Maria Tsimpoukelli, Mathew Oldham, Mathieu Rita, Maya Pavlova, Melanie Kambadur, Mike Lewis, Min Si, Mitesh Kumar Singh, Mona Hassan, Naman Goyal, Narjes Torabi, Nikolay Bashlykov, Nikolay Bogoychev, Niladri Chatterji, Ning Zhang, Olivier Duchenne, Onur Çelebi, Patrick Alrassy, Pengchuan Zhang, Pengwei Li, Petar Vasic, Peter Weng, Prajjwal Bhargava, Pratik Dubal, Praveen Krishnan, Punit Singh Koura, Puxin Xu, Qing He, Qingxiao Dong, Ragavan Srinivasan, Raj Ganapathy, Ramon Calderer, Ricardo Silveira Cabral, Robert Stojnic, Roberta Raileanu, Rohan Maheswari, Rohit Girdhar, Rohit Patel, Romain Sauvestre, Ronnie Polidoro, Roshan Sumbaly, Ross Taylor, Ruan Silva, Rui Hou, Rui Wang, Saghar Hosseini, Sahana Chennabasappa, Sanjay Singh, Sean Bell, Seohyun Sonia Kim, Sergey Edunov, Shaoliang Nie, Sharan Narang, Sharath Raparthy, Sheng Shen, Shengye Wan, Shruti Bhosale, Shun Zhang, Simon Vandenhende, Soumya Batra, Spencer Whitman, Sten Sootla, Stephane Collot, Suchin Gururangan, Sydney Borodinsky, Tamar Herman, Tara Fowler, Tarek Sheasha, Thomas Georgiou, Thomas Scialom, Tobias Speckbacher, Todor Mihaylov, Tong Xiao, Ujjwal Karn, Vedanuj Goswami, Vibhor Gupta, Vignesh Ramanathan, Viktor Kerkez, Vincent Gonguet, Virginie Do, Vish Vogeti, Vitor Albiero, Vladan Petrovic, Weiwei Chu, Wenhan Xiong, Wenyin Fu, Whitney Meers, Xavier Martinet, Xiaodong Wang, Xiaofang Wang, Xiaoqing Ellen Tan, Xide Xia, Xinfeng Xie, Xuchao Jia, Xuwei Wang, Yaelle Goldschlag, Yashesh Gaur, Yasmine Babaei, Yi Wen, Yiwen Song, Yuchen Zhang, Yue Li, Yuning Mao, Zacharie Delpierre Coudert, Zheng Yan, Zhengxing Chen, Zoe Papakipos, Aaditya Singh, Aayushi Srivastava, Abha Jain, Adam Kelsey, Adam Shajnfeld, Adithya Gangidi, Adolfo Victoria, Ahuva Goldstand, Ajay Menon, Ajay Sharma, Alex Boesenberg, Alexei Baevski, Allie Feinstein, Amanda Kallet, Amit Sangani, Amos Teo, Anam Yunus, Andrei Lupu, Andres Alvarado, Andrew Caples, Andrew Gu, Andrew Ho, Andrew Poulton, Andrew Ryan, Ankit Ramchandani, Annie Dong, Annie Franco, Anuj Goyal, Aparajita Saraf, Arkabandhu Chowdhury, Ashley Gabriel, Ashwin Bharambe, Assaf Eisenman, Azadeh Yazdan, Beau James, Ben Maurer, Benjamin Leonhardi, Bernie Huang, Beth Loyd, Beto De Paola, Bhargavi Paranjape, Bing Liu, Bo Wu, Boyu Ni, Braden Hancock, Bram Wasti, Brandon Spence, Brani Stojkovic, Brian Gamido, Britt Montalvo, Carl Parker, Carly Burton, Catalina Mejia, Ce Liu, Changhan Wang, Changkyu Kim, Chao Zhou, Chester Hu, Ching-Hsiang Chu, Chris Cai, Chris Tindal, Christoph Feichtenhofer, Cynthia Gao, Damon Civin, Dana Beaty, Daniel Kreymer, Daniel Li, David Adkins, David Xu, Davide Testuggine, Delia David, Devi Parikh, Diana Liskovich, Didem Foss, Dingkang Wang, Duc Le, Dustin Holland, Edward Dowling, Eissa Jamil, Elaine Montgomery, Eleonora Presani, Emily Hahn, Emily Wood, Eric-Tuan Le, Erik Brinkman, Esteban Arcaute, Evan Dunbar, Evan Smothers, Fei Sun, Felix Kreuk, Feng Tian, Filippos Kokkinos, Firat Ozgenel, Francesco Caggioni, Frank Kanayet, Frank Seide, Gabriela Medina Florez, Gabriella Schwarz, Gada Badeer, Georgia Swee, Gil Halpern, Grant Herman, Grigory Sizov, Guangyi, Zhang, Guna Lakshminarayanan, Hakan Inan, Hamid Shojanazeri, Han Zou, Hannah Wang, Hanwen Zha, Haroun Habeeb, Harrison Rudolph, Helen Suk, Henry Aspegen, Hunter Goldman, Hongyuan Zhan, Ibrahim Damlaj, Igor Molybog, Igor Tufanov, Ilias Leontiadis, Irina-Elena Veliche, Itai Gat, Jake Weissman, James Geboski, James Kohli, Janice Lam, Japhet Asher, Jean-Baptiste Gaya, Jeff Marcus, Jeff Tang, Jennifer Chan, Jenny Zhen, Jeremy Reizenstein, Jeremy Teboul, Jessica Zhong, Jian Jin, Jingyi Yang, Joe Cummings, Jon Carvill, Jon Shepard, Jonathan McPhie, Jonathan Torres, Josh Ginsburg, Junjie Wang, Kai Wu, Kam Hou U, Karan Saxena, Kartikay Khandelwal, Katayoun Zand, Kathy Matosich, Kaushik Veeraraghavan, Kelly Michelena, Keqian Li, Kiran Jagadeesh, Kun Huang, Kunal Chawla, Kyle Huang, Lailin Chen, Lakshya Garg, Lavender A, Leandro Silva, Lee Bell, Lei Zhang, Liangpeng Guo, Licheng Yu, Liron Moshkovich, Luca Wehrstedt, Madian Khabsa, Manav Avalani, Manish Bhatt, Martynas Mankus, Matan Hasson, Matthew Lennie, Matthias Reso, Maxim Groshev, Maxim Naumov, Maya Lathi, Meghan Keneally, Miao Liu, Michael L. Seltzer, Michal Valko, Michelle Restrepo, Mihir Patel, Mik Vyatskov, Mikayel Samvelyan, Mike Clark, Mike Macey, Mike Wang, Miquel Jubert Hermoso, Mo Metanat, Mohammad Rastegari, Munish Bansal, Nandhini Santhanam, Natascha Parks, Natasha White, Navyata Bawa, Nayan Singhal, Nick Egebo, Nicolas Usunier, Nikhil Mehta, Nikolay Pavlovich Laptev, Ning Dong, Norman Cheng, Oleg Chernoguz, Olivia Hart, Omkar Salpekar, Ozlem Kalinli, Parkin Kent, Parth Parekh, Paul Saab, Pavan Balaji, Pedro Rittner, Philip Bontrager, Pierre Roux, Piotr Dollar, Polina Zvyagina, Prashant Ratanchandani, Pritish Yuvraj, Qian Liang, Rachad Alao, Rachel Rodriguez, Rafi Ayub, Raghotham Murthy, Raghu Nayani, Rahul Mitra, Rangaprabhu Parthasarathy,

Raymond Li, Rebekkah Hogan, Robin Battey, Rocky Wang, Russ Howes, Ruty Rinott, Sachin Mehta, Sachin Siby, Sai Jayesh Bondu, Samyak Datta, Sara Chugh, Sara Hunt, Sargun Dhillon, Sasha Sidorov, Satadru Pan, Saurabh Mahajan, Saurabh Verma, Seiji Yamamoto, Sharadh RamaSwamy, Shaun Lindsay, Shaun Lindsay, Sheng Feng, Shenghao Lin, Shengxin Cindy Zha, Shishir Patil, Shiva Shankar, Shuqiang Zhang, Shuqiang Zhang, Sinong Wang, Sneha Agarwal, Soji Sajuyigbe, Soumith Chintala, Stephanie Max, Stephen Chen, Steve Kehoe, Steve Satterfield, Sudarshan Govindaprasad, Sumit Gupta, Summer Deng, Sungmin Cho, Sunny Virk, Suraj Subramanian, Sy Choudhury, Sydney Goldman, Tal Remez, Tamar Glaser, Tamara Best, Thilo Koehler, Thomas Robinson, Tianhe Li, Tianjun Zhang, Tim Matthews, Timothy Chou, Tzook Shaked, Varun Vontimitta, Victoria Ajayi, Victoria Montanez, Vijai Mohan, Vinay Satish Kumar, Vishal Mangla, Vlad Ionescu, Vlad Poenaru, Vlad Tiberiu Mihăilescu, Vladimir Ivanov, Wei Li, Wencheng Wang, Wenwen Jiang, Wes Bouaziz, Will Constable, Xiaocheng Tang, Xiaojian Wu, Xiaolan Wang, Xilun Wu, Xinbo Gao, Yaniv Kleinman, Yanjun Chen, Ye Hu, Ye Jia, Ye Qi, Yenda Li, Yilin Zhang, Ying Zhang, Yossi Adi, Youngjin Nam, Yu, Wang, Yu Zhao, Yuchen Hao, Yundi Qian, Yunlu Li, Yuzi He, Zach Rait, Zachary DeVito, Zef Rosnbrick, Zhao-duo Wen, Zhenyu Yang, Zhiwei Zhao, and Zhiyu Ma. The llama 3 herd of models, 2024. URL <https://arxiv.org/abs/2407.21783>.

Jonathan Ho, Ajay Jain, and Pieter Abbeel. Denoising diffusion probabilistic models, 2020. URL <https://arxiv.org/abs/2006.11239>.

Tero Karras, Samuli Laine, Miika Aittala, Janne Hellsten, Jaakko Lehtinen, and Timo Aila. Analyzing and improving the image quality of stylegan, 2020. URL <https://arxiv.org/abs/1912.04958>.

John Kirchenbauer, Jonas Geiping, Yuxin Wen, Jonathan Katz, Ian Miers, and Tom Goldstein. A watermark for large language models, 2024. URL <https://arxiv.org/abs/2301.10226>.

Tsung-Yi Lin, Priya Goyal, Ross Girshick, Kaiming He, and Piotr Dollár. Focal loss for dense object detection, 2018. URL <https://arxiv.org/abs/1708.02002>.

Stephen Merity, Caiming Xiong, James Bradbury, and Richard Socher. Pointer sentinel mixture models, 2016. URL <https://arxiv.org/abs/1609.07843>.

OpenAI, Josh Achiam, Steven Adler, Sandhini Agarwal, Lama Ahmad, Ilge Akkaya, Florencia Leoni Aleman, Diogo Almeida, Janko Altenschmidt, Sam Altman, Shyamal Anadkat, Red Avila, Igor Babuschkin, Suchir Balaji, Valerie Balcom, Paul Baltescu, Haiming Bao, Mohammad Bavarian, Jeff Belgum, Irwan Bello, Jake Berdine, Gabriel Bernadett-Shapiro, Christopher Berner, Lenny Bogdonoff, Oleg Boiko, Madelaine Boyd, Anna-Luisa Brakman, Greg Brockman, Tim Brooks, Miles Brundage, Kevin Button, Trevor Cai, Rosie Campbell, Andrew Cann, Brittany Carey, Chelsea Carlson, Rory Carmichael, Brooke Chan, Che Chang, Fotis Chantzis, Derek Chen, Sully Chen, Ruby Chen, Jason Chen, Mark Chen, Ben Chess, Chester Cho, Casey Chu, Hyung Won Chung, Dave Cummings, Jeremiah Currier, Yunxing Dai, Cory Decareaux, Thomas Degry, Noah Deutscher, Damien Deville, Arka Dhar, David Dohan, Steve Dowling, Sheila Dunning, Adrien Ecoffet, Atty Eleti, Tyna Eloundou, David Farhi, Liam Fedus, Niko Felix, Simón Posada Fishman, Juston Forte, Isabella Fulford, Leo Gao, Elie Georges, Christian Gibson, Vik Goel, Tarun Gogineni, Gabriel Goh, Rapha Gontijo-Lopes, Jonathan Gordon, Morgan Grafstein, Scott Gray, Ryan Greene, Joshua Gross, Shixiang Shane Gu, Yufei Guo, Chris Hallacy, Jesse Han, Jeff Harris, Yuchen He, Mike Heaton, Johannes Heidecke, Chris Hesse, Alan Hickey, Wade Hickey, Peter Hoeschele, Brandon Houghton, Kenny Hsu, Shengli Hu, Xin Hu, Joost Huizinga, Shantanu Jain, Shawn Jain, Joanne Jang, Angela Jiang, Roger Jiang, Haozhun Jin, Denny Jin, Shino Jomoto, Billie Jonn, Heewoo Jun, Tomer Kaftan, Łukasz Kaiser, Ali Kamali, Ingmar Kanitscheider, Nitish Shirish Keskar, Tabarak Khan, Logan Kilpatrick, Jong Wook Kim, Christina Kim, Yongjik Kim, Jan Hendrik Kirchner, Jamie Kiros, Matt Knight, Daniel Kokotajlo, Łukasz Kondraciuk, Andrew Kondrich, Aris Konstantinidis, Kyle Kosic, Gretchen Krueger, Vishal Kuo, Michael Lampe, Ikai Lan, Teddy Lee, Jan Leike, Jade Leung, Daniel Levy, Chak Ming Li, Rachel Lim, Molly Lin, Stephanie Lin, Mateusz Litwin, Theresa Lopez, Ryan Lowe, Patricia Lue, Anna Makanju, Kim Malfacini, Sam Manning, Todor Markov, Yaniv Markovski, Bianca Martin, Katie Mayer, Andrew Mayne, Bob McGrew, Scott Mayer McKinney, Christine McLeavey, Paul McMillan, Jake McNeil, David Medina, Aalok Mehta, Jacob Menick, Luke Metz, Andrey Mishchenko, Pamela Mishkin, Vinnie Monaco, Evan Morikawa, Daniel

Mossing, Tong Mu, Mira Murati, Oleg Murk, David Mély, Ashvin Nair, Reiichiro Nakano, Rajeev Nayak, Arvind Neelakantan, Richard Ngo, Hyeonwoo Noh, Long Ouyang, Cullen O’Keefe, Jakub Pachocki, Alex Paino, Joe Palermo, Ashley Pantuliano, Giambattista Parascandolo, Joel Parish, Emy Parparita, Alex Passos, Mikhail Pavlov, Andrew Peng, Adam Perelman, Filipe de Avila Belbute Peres, Michael Petrov, Henrique Ponde de Oliveira Pinto, Michael, Pokorny, Michelle Pokrass, Vitchyr H. Pong, Tolly Powell, Alethea Power, Boris Power, Elizabeth Proehl, Raul Puri, Alec Radford, Jack Rae, Aditya Ramesh, Cameron Raymond, Francis Real, Kendra Rimbach, Carl Ross, Bob Rotsted, Henri Roussez, Nick Ryder, Mario Saltarelli, Ted Sanders, Shibani Santurkar, Girish Sastry, Heather Schmidt, David Schnurr, John Schulman, Daniel Sel-sam, Kyla Sheppard, Toki Sherbakov, Jessica Shieh, Sarah Shoker, Pranav Shyam, Szymon Sidor, Eric Sigler, Maddie Simens, Jordan Sitkin, Katarina Slama, Ian Sohl, Benjamin Sokolowsky, Yang Song, Natalie Staudacher, Felipe Petroski Such, Natalie Summers, Ilya Sutskever, Jie Tang, Nikolas Tezak, Madeleine B. Thompson, Phil Tillet, Amin Tootoonchian, Elizabeth Tseng, Preston Tuggle, Nick Turley, Jerry Tworek, Juan Felipe Cerón Uribe, Andrea Vallone, Arun Vijayvergiya, Chelsea Voss, Carroll Wainwright, Justin Jay Wang, Alvin Wang, Ben Wang, Jonathan Ward, Jason Wei, CJ Weinmann, Akila Welihinda, Peter Welinder, Jiayi Weng, Lilian Weng, Matt Wiethoff, Dave Willner, Clemens Winter, Samuel Wolrich, Hannah Wong, Lauren Workman, Sherwin Wu, Jeff Wu, Michael Wu, Kai Xiao, Tao Xu, Sarah Yoo, Kevin Yu, Qiming Yuan, Wojciech Zaremba, Rowan Zellers, Chong Zhang, Marvin Zhang, Shengjia Zhao, Tianhao Zheng, Juntang Zhuang, William Zhuk, and Barret Zoph. Gpt-4 technical report, 2024. URL <https://arxiv.org/abs/2303.08774>.

Aditya Ramesh, Mikhail Pavlov, Gabriel Goh, Scott Gray, Chelsea Voss, Alec Radford, Mark Chen, and Ilya Sutskever. Zero-shot text-to-image generation, 2021. URL <https://arxiv.org/abs/2102.12092>.

Daniele Rege Cambrin, Giuseppe Gallipoli, Irene Benedetto, Luca Cagliero, and Paolo Garza. Beyond accuracy optimization: Computer vision losses for large language model fine-tuning. In *Findings of the Association for Computational Linguistics: EMNLP 2024*, pp. 12060–12079. Association for Computational Linguistics, 2024. doi: 10.18653/v1/2024.findings-emnlp.704. URL <http://dx.doi.org/10.18653/v1/2024.findings-emnlp.704>.

Chitwan Saharia, William Chan, Saurabh Saxena, Lala Li, Jay Whang, Emily Denton, Seyed Kamalar Seyed Ghasemipour, Burcu Karagol Ayan, S. Sara Mahdavi, Rapha Gontijo Lopes, Tim Salimans, Jonathan Ho, David J Fleet, and Mohammad Norouzi. Photorealistic text-to-image diffusion models with deep language understanding, 2022. URL <https://arxiv.org/abs/2205.11487>.

Rylan Schaeffer, Joshua Kazdan, Alvan Caleb Arulandu, and Sanmi Koyejo. Position: Model collapse does not mean what you think, 2025. URL <https://arxiv.org/abs/2503.03150>.

I. Shumailov, Z. Shumaylov, and Y. Zhao. Ai models collapse when trained on recursively generated data. *NNature* 631, 755–759 (2024), 2024a. doi: <https://doi.org/10.1038/s41586-024-07566-y>.

Ilia Shumailov, Zakhar Shumaylov, Yiren Zhao, Yarin Gal, Nicolas Papernot, and Ross Anderson. The curse of recursion: Training on generated data makes models forget, 2024b. URL <https://arxiv.org/abs/2305.17493>.

Gemma Team, Aishwarya Kamath, Johan Ferret, Shreya Pathak, Nino Vieillard, Ramona Merhej, Sarah Perrin, Tatiana Matejovicova, Alexandre Ramé, Morgane Rivière, Louis Rouillard, Thomas Mesnard, Geoffrey Cideron, Jean bastien Grill, Sabela Ramos, Edouard Yvinec, Michelle Casbon, Etienne Pot, Ivo Penchev, Gaël Liu, Francesco Visin, Kathleen Kenealy, Lucas Beyer, Xiaohai Zhai, Anton Tsitsulin, Robert Busa-Fekete, Alex Feng, Noveen Sachdeva, Benjamin Coleman, Yi Gao, Basil Mustafa, Iain Barr, Emilio Parisotto, David Tian, Matan Eyal, Colin Cherry, Jan-Thorsten Peter, Danila Sinopalnikov, Surya Bhupatiraju, Rishabh Agarwal, Mehran Kazemi, Dan Malkin, Ravin Kumar, David Vilar, Idan Brusilovsky, Jiaming Luo, Andreas Steiner, Abe Friesen, Abhanshu Sharma, Abheesht Sharma, Adi Mayrav Gilady, Adrian Goedeckemeyer, Alaa Saade, Alex Feng, Alexander Kolesnikov, Alexei Bendebury, Alvin Abdagic, Amit Vadi, András György, André Susano Pinto, Anil Das, Ankur Bapna, Antoine Miech, Antoine Yang, Antonia Paterson, Ashish Shenoy, Ayan Chakrabarti, Bilal Piot, Bo Wu, Bobak Shahriari, Bryce Petrini, Charlie Chen, Charline Le Lan, Christopher A. Choquette-Choo, CJ Carey, Cormac Brick, Daniel

Deutsch, Danielle Eisenbud, Dee Cattle, Derek Cheng, Dimitris Paparas, Divyashree Shivakumar Sreepathihalli, Doug Reid, Dustin Tran, Dustin Zelle, Eric Noland, Erwin Huizenga, Eugene Kharitonov, Frederick Liu, Gagik Amirkhanyan, Glenn Cameron, Hadi Hashemi, Hanna Klimczak-Plucińska, Harman Singh, Harsh Mehta, Harshal Tushar Lehri, Hussein Hazimeh, Ian Ballantyne, Idan Szpektor, Ivan Nardini, Jean Pouget-Abadie, Jetha Chan, Joe Stanton, John Weting, Jonathan Lai, Jordi Orbay, Joseph Fernandez, Josh Newlan, Ju yeong Ji, Jyotinder Singh, Kat Black, Kathy Yu, Kevin Hui, Kiran Vodrahalli, Klaus Greff, Linhai Qiu, Marcella Valentine, Marina Coelho, Marvin Ritter, Matt Hoffman, Matthew Watson, Mayank Chaturvedi, Michael Moynihan, Min Ma, Nabila Babar, Natasha Noy, Nathan Byrd, Nick Roy, Nikola Momchev, Nilay Chauhan, Noveen Sachdeva, Oskar Bunyan, Pankil Botarda, Paul Caron, Paul Kishan Rubenstein, Phil Culliton, Philipp Schmid, Pier Giuseppe Sessa, Pingmei Xu, Piotr Stanczyk, Pouya Tafti, Rakesh Shivanna, Renjie Wu, Renke Pan, Reza Rokni, Rob Willoughby, Rohith Vallu, Ryan Mullins, Sammy Jerome, Sara Smoot, Sertan Girgin, Shariq Iqbal, Shashir Reddy, Shruti Sheth, Siim Pöder, Sijal Bhatnagar, Sindhu Raghuram Panyam, Sivan Eiger, Susan Zhang, Tianqi Liu, Trevor Yacovone, Tyler Liechty, Uday Kalra, Utku Evcı, Vedant Misra, Vincent Roseberry, Vlad Feinberg, Vlad Kolesnikov, Woohyun Han, Woosuk Kwon, Xi Chen, Yinlam Chow, Yuvein Zhu, Zichuan Wei, Zoltan Egyed, Victor Cotruta, Minh Giang, Phoebe Kirk, Anand Rao, Kat Black, Nabila Babar, Jessica Lo, Erica Moreira, Luiz Gustavo Martins, Omar Sanseviero, Lucas Gonzalez, Zach Gleicher, Tris Warkentin, Vahab Mirrokni, Evan Senter, Eli Collins, Joelle Barra, Zoubin Ghahramani, Raia Hadsell, Yossi Matias, D. Sculley, Slav Petrov, Noah Fiedel, Noam Shazeer, Oriol Vinyals, Jeff Dean, Demis Hassabis, Koray Kavukcuoglu, Clement Farabet, Elena Buchatskaya, Jean-Baptiste Alayrac, Rohan Anil, Dmitry Lepikhin, Sebastian Borgeaud, Olivier Bachem, Armand Joulin, Alek Andreev, Cassidy Hardin, Robert Dadashi, and Léonard Hussenot. Gemma 3 technical report, 2025. URL <https://arxiv.org/abs/2503.19786>.

Pablo Villalobos, Anson Ho, Jaime Sevilla, Tamay Besiroglu, Lennart Heim, and Marius Hobbahn. Will we run out of data? limits of llm scaling based on human-generated data, 2024. URL <https://arxiv.org/abs/2211.04325>.

Alex Warstadt, Alicia Parrish, Haokun Liu, Anhad Mohananey, Wei Peng, Sheng-Fu Wang, and Samuel R. Bowman. Blimp: The benchmark of linguistic minimal pairs for english, 2023. URL <https://arxiv.org/abs/1912.00582>.

Rowan Zellers, Ari Holtzman, Yonatan Bisk, Ali Farhadi, and Yejin Choi. Hellaswag: Can a machine really finish your sentence?, 2019. URL <https://arxiv.org/abs/1905.07830>.

Ruiqi Zhang and Farinaz Koushanfar. Emmark: Robust watermarks for ip protection of embedded quantized large language models, 2024. URL <https://arxiv.org/abs/2402.17938>.

A APPENDIX

APPENDIX A FOCAL LOSS

To complement the main results, we additionally evaluated Focal Loss (FL) in our self-consuming generation framework. While the core paper focuses on Cross Entropy (CE), Truncated Cross Entropy (TCE), and their performance trade-offs, we found it instructive to include FL due to its growing interest in generative modeling. FL shares with TCE the goal of down-weighting confident predictions, which may help preserve the tail of the token distribution during continued generation.

Focal Loss (FL), originally introduced for addressing class imbalance in image segmentation tasks Lin et al. (2018), emphasizes hard, misclassified examples. It is defined as:

$$FL(p_t) = -(1 - p_t)^\gamma \times \log(p_t)$$

where p_t is the probability of the correct class, and γ is a tunable hyperparameter that controls the down-weighting of well-classified samples. FL reduces the loss for confident predictions, acting similarly to cross-entropy on uncertain examples, thus helping avoid overfitting to self-generated tokens.

Recent work Rege Cambrin et al. (2024) has shown FL’s effectiveness in language modeling, outperforming CE on commonsense reasoning and math tasks. In the context of this work, FL aligns with our objective of mitigating model collapse by emphasizing rare token learning and preserving the tail of the output distribution.

Figure 8 presents the total Knowledge Retention (KR-total) accuracy across generations for LLaMA-3.2-1B on WikiText. TCE maintains high performance throughout training, while CE exhibits significant degradation. FL performs comparably to TCE in early stages but begins to degrade slightly earlier, indicating less robustness over long sequences of regeneration.

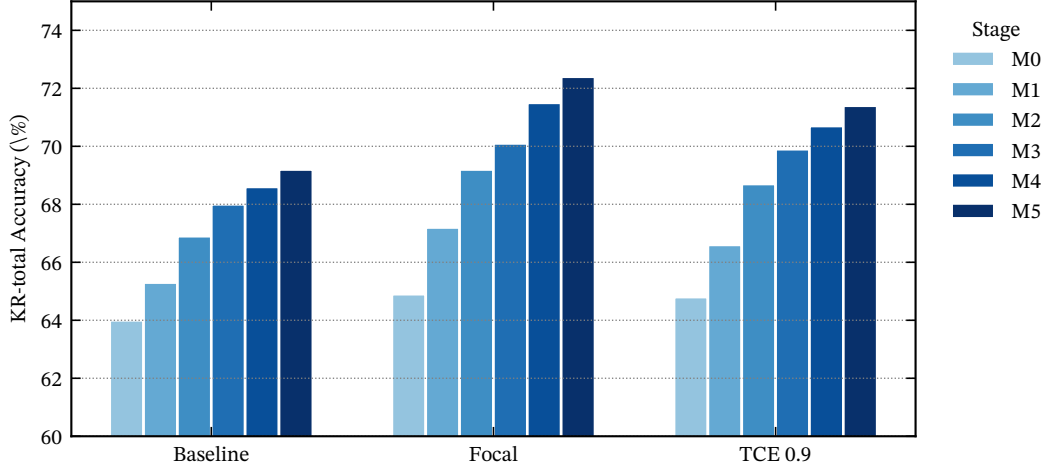


Figure 8: Total knowledge retention (KR-total) accuracy with LLaMA-3.2-1B model trained on WikiText. TCE retains learning capability and even exceeds the baseline throughout different stages.

We quantify robustness by measuring each model’s *time to failure*—defined as the number of generations before KR accuracy falls below 75%. As shown in Figure 9, CE fails between the first and second stages, while FL extends time to failure by over 1.5 \times , and TCE pushes this boundary even further to over 2.3 \times . These results suggest that while FL partially delays collapse, TCE remains the most effective at sustaining meaningful retention under compounding self-generation.

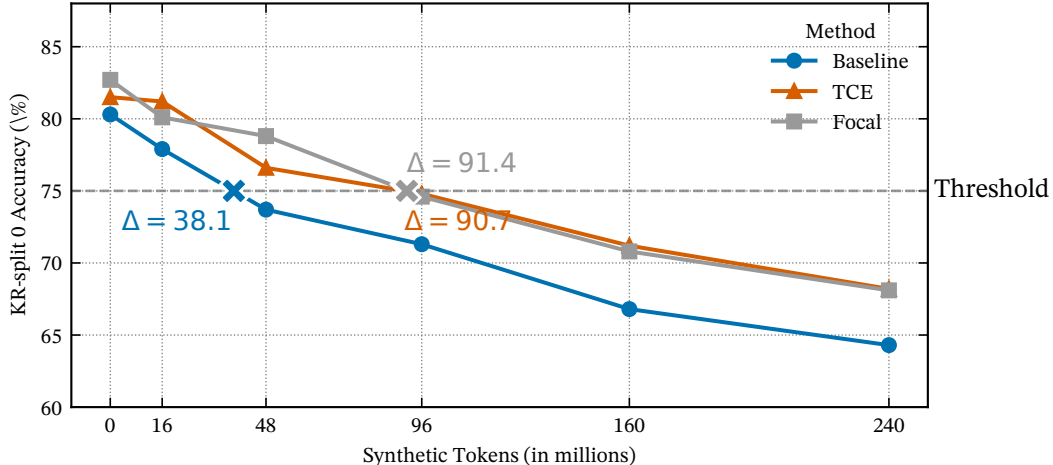


Figure 9: Time-to-failure comparison of loss functions on synthetic subsets of WikiText. Dotted red lines indicate failure threshold (75% KR accuracy). FL delays collapse relative to CE, while TCE offers the strongest retention.

To evaluate distributional fidelity, we tracked the KL divergence between generated outputs and the original training distribution. Figure 10 demonstrates that CE leads to rapid divergence, indicative of distributional drift and collapse. FL moderately slows this drift, whereas TCE consistently maintains low divergence across generations, reinforcing its effectiveness in preserving output diversity and alignment.

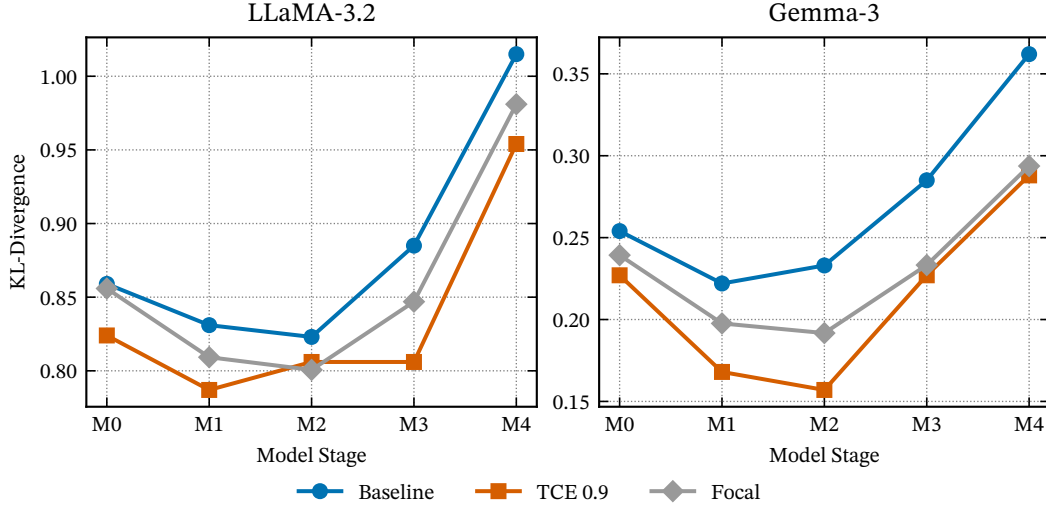


Figure 10: KL divergence across generations between model outputs and the original training distribution. FL moderates divergence growth compared to CE, while TCE consistently preserves distributional fidelity.

APPENDIX B KNOWLEDGE RETENTION TEST

KR test is a straightforward tool for evaluating models on dataset specific facts. Our KR-test of Wikitext consists of paragraphs (i.e. contexts) followed by two completions, one with true facts based on the Wikitext and another with major flaws in the factual parts. An example of this dataset is shown in Table 5.

Table 5: Example KR-test question generated from Wikitext. The model is given a context and must assign higher probability to the factually correct completion.

Wikitext:

South of Heaven is the fourth studio album by American thrash metal band Slayer . Released on July 5 , 1988 , the album was the band 's second collaboration with record producer Rick Rubin ...

Context:

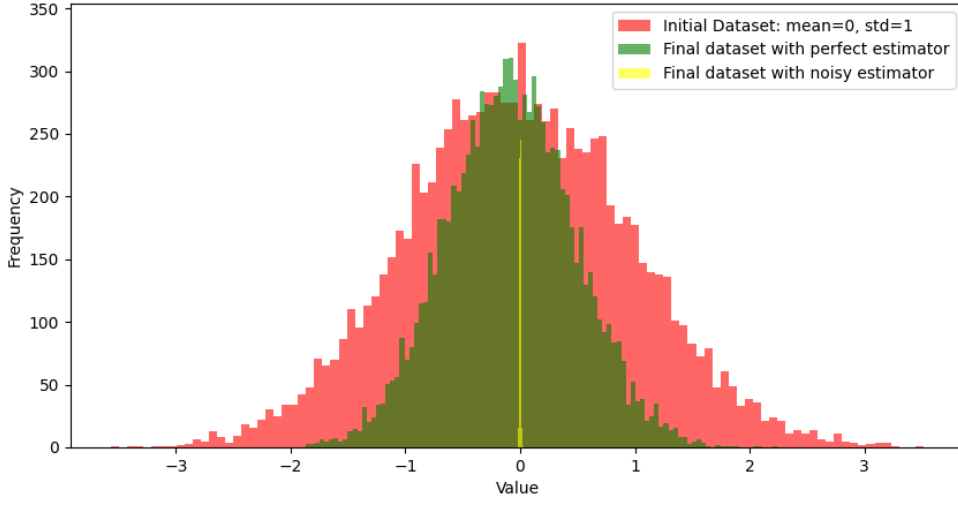
South of Heaven is the fourth studio album by American thrash metal band Slayer , released on July 5 , 1988.

True Sentence:

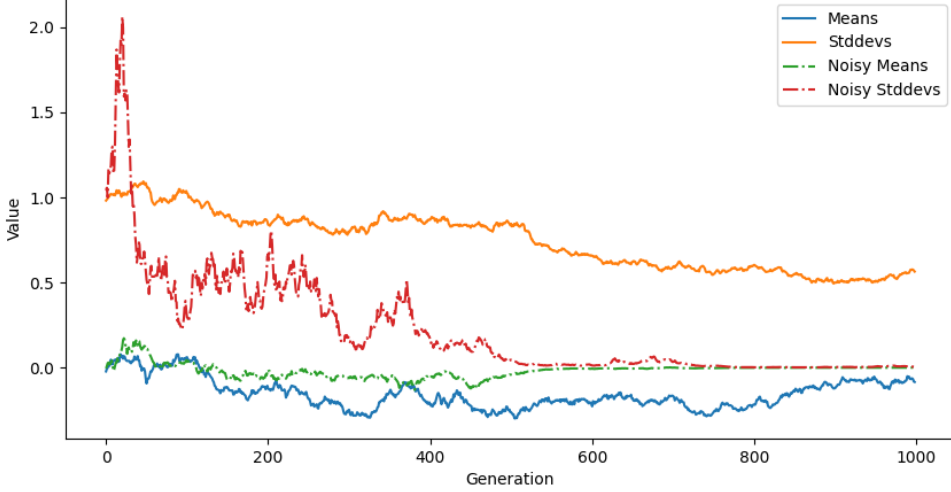
The album marked Slayer 's second collaboration with producer Rick Rubin .

False Sentence:

The album marked Slayer 's first collaboration with producer Rick Rubin .



(a) Histogram of distributions



(b) Mean and standard deviation of estimators

Figure 11: Example of model collapse on single dimensional Gaussian data with Maximum Likelihood Estimators (MLE). (a) The probable outcomes are over-estimated and rare events start to vanish; this is also known as the disappearance of the tails of distributions. (b) The noisy estimator (green) collapses in 1000 generations as the standard deviation converges to zero, but the perfect estimator (purple) drifts slightly from the original distribution.

APPENDIX C INEVITABLE MODEL COLLAPSE

As a toy example, we demonstrate this issue using a single dimensional Gaussian distribution and use two sets of estimators, one perfect and the other noisy in Fig 11. Using a perfect estimator (left) the newly generated datasets are less severely affected. However, given enough time, the model collapse would still occur. Model Collapse happens rapidly with an imperfect estimator (right) using single dimensional Gaussian dataset. The tails of the original distribution have completely disappeared due to finite sampling and functional approximation errors.

The MLE estimators for a Gaussian distribution are

$$\hat{\mu} = \frac{1}{N} \sum_{i=1}^N x_i, \hat{\sigma}^2 = \frac{1}{n}$$

and this is used as the perfect estimator. For the noisy estimator, simply a noise $w \sim \mathcal{N}(0, 1)$ has been added to the estimators.

The aforementioned issue is presented in Fig 11 where Model Collapse occurs while using the perfect estimator. However, compared to a noisy estimator it has drifted less from the original distribution showing the importance of learning underrepresented samples.

APPENDIX D COMPREHENSIVE EVALUATION RESULTS

In this section we discuss the evaluation results from every stage of aforementioned experiments. These results include Baseline (CE), Focal Loss, and two variations of Truncated Cross Entropy that we found to be competitive.

D.1 WIKITEXT RESULTS

Table 6 presents the unified benchmark results of LLaMA across six recursive training stages on the WikiText dataset. At the initial stage (M0), both Focal loss and TCE (0.9) improve accuracy compared to the baseline across most tasks, with TCE slightly outperforming Focal in Blimp and GSM8k. As training progresses, all methods experience performance degradation, consistent with model collapse dynamics; however, Focal and TCE maintain significantly higher accuracies than the baseline, especially in later stages (M3–M5). Notably, Focal loss consistently achieves the best or second-best scores on Hellaswag and KR-split 0, while TCE often excels on Blimp and GSM8k. This demonstrates that both confidence-aware losses are effective at mitigating performance decay in recursive synthetic training.

Table 6: LLaMA-3.2-1B unified benchmark results across Blimp, Hellaswag, GSM8k, KR-split 0, and KR-total of trainings on WikiText. For ease of readability, we highlight the highest accuracy in bold and the second best as underlined.

| Stage | Method | Blimp | Hellaswag | GSM8k | KR-split 0 | KR-total |
|-------|------------------------|--------------|--------------|-------------|--------------|--------------|
| M0 | Baseline | 75.1% | 58.5% | 2.5% | 80.3% | 64.0% |
| | Focal ($\gamma = 2$) | <u>75.5%</u> | 62.5% | <u>2.8%</u> | 82.7% | 64.9% |
| | TCE 0.9 | 76.8% | <u>61.8%</u> | 2.9% | 81.5% | <u>64.8%</u> |
| | TCE 0.99 | 75.5% | 59.9% | 2.5% | <u>81.7%</u> | 64.0% |
| M1 | Baseline | 70.5% | 56.1% | 1.8% | 77.9% | 65.3% |
| | Focal ($\gamma = 2$) | 74.9% | 59.9% | <u>2.1%</u> | <u>80.1%</u> | 67.2% |
| | TCE 0.9 | 71.8% | <u>59.2%</u> | 2.2% | 81.2% | <u>66.6%</u> |
| | TCE 0.99 | <u>73.3%</u> | 57.1% | 1.2% | 78.5% | 65.1% |
| M2 | Baseline | 66.1% | 52.25% | 1.8% | 73.7% | 66.9% |
| | Focal ($\gamma = 2$) | 72.8% | 55.8% | <u>1.6%</u> | 78.8% | 69.2% |
| | TCE 0.9 | <u>70.4%</u> | <u>54.4%</u> | 1.2% | 76.6% | <u>68.7%</u> |
| | TCE 0.99 | 67.1% | 53.4% | 1.5% | <u>76.8%</u> | 67.6% |
| M3 | Baseline | 62.5% | 49.2% | 1.6% | 71.3% | 68.0% |
| | Focal ($\gamma = 2$) | 72.3% | 53.0% | 1.1% | <u>74.6%</u> | 70.1% |
| | TCE 0.9 | 68.5% | <u>51.6%</u> | 0.9% | 74.8% | <u>69.9%</u> |
| | TCE 0.99 | 66.8% | 50.6% | <u>1.2%</u> | 72.5% | <u>69.9%</u> |
| M4 | Baseline | 66.8% | 47.1% | <u>0.7%</u> | 66.8% | 68.6% |
| | Focal ($\gamma = 2$) | 71.3% | 50.8% | <u>0.6%</u> | <u>70.8%</u> | 71.5% |
| | TCE 0.9 | 68.3% | <u>49.8%</u> | 0.8% | 71.2% | <u>70.7%</u> |
| | TCE 0.99 | <u>69.9%</u> | 48.3% | <u>0.7%</u> | 69.1% | 70.4% |
| M5 | Baseline | 63.3% | 45.7% | <u>1%</u> | 64.3% | 69.2% |
| | Focal ($\gamma = 2$) | 67.5% | 49.6% | 1.1% | <u>68.1%</u> | 72.4% |
| | TCE 0.9 | <u>63.6%</u> | <u>48.4%</u> | 0.9% | 68.2% | <u>71.4%</u> |
| | TCE 0.99 | 62.6% | 46.9% | 0.8% | 66.2% | 70.2% |

Table 7 summarizes the Gemma model’s benchmark results across six training stages on WikiText. At M0, TCE (0.9) and TCE (0.99) achieve the highest accuracies in Blimp, GSM8k, and KR metrics, indicating a strong start for TCE variants. Throughout the stages, Focal loss shows stable performance across most tasks, with improvements in Hellaswag and KR-split 0 in later stages (M3–M5), while TCE (0.9) and (0.99) continue to deliver competitive or superior scores on Blimp and GSM8k. These results confirm that confidence-aware objectives help preserve performance during recursive training, with TCE offering a slight advantage in certain metrics.

Table 7: Gemma-3-1b-pt unified benchmark results across Blimp, Hellaswag, GSM8k, KR-split 0, and KR-total of trainings on Wikitext

| Stage | Method | Blimp | Hellaswag | GSM8k | KR-split 0 | KR-total |
|-------|----------|--------------|--------------|-------------|--------------|--------------|
| M0 | Baseline | 71.2% | 63.9% | 1.1% | 78.5% | <u>67.7%</u> |
| | Focal | <u>73.5%</u> | 64.9% | 0.7% | 78% | <u>67.4%</u> |
| | TCE 0.9 | 73.9% | 64.6% | <u>1.5%</u> | 79.7% | 68.2% |
| | TCE 0.99 | 71.5% | 64.1% | 1.7% | <u>79.5%</u> | 67.4% |
| M1 | Baseline | 68.2% | 59.1% | 1.2% | 74.6% | 70.9% |
| | Focal | <u>70.9%</u> | <u>60%</u> | 1.2% | 74.9% | 71.3% |
| | TCE 0.9 | 70.6% | 60.5% | 1% | 77.2% | 72.1% |
| | TCE 0.99 | 73.2% | 59.7% | <u>1.1%</u> | <u>75.1%</u> | <u>72%</u> |
| M2 | Baseline | 67% | 56% | 0.8% | <u>73.8%</u> | 74.7% |
| | Focal | <u>67.1%</u> | 58.4% | 1.1% | 75.2% | <u>76.7%</u> |
| | TCE 0.9 | 70.4% | <u>57.7%</u> | 0.8% | 75.2% | 76.9% |
| | TCE 0.99 | <u>69%</u> | 56.7% | 0.8% | 73.3% | 75.3% |
| M3 | Baseline | 62.9% | 55.2% | 1.4% | 72.1% | 72.5% |
| | Focal | <u>66.2%</u> | 56.1% | 1.2% | <u>72.7%</u> | <u>73.4%</u> |
| | TCE 0.9 | 65.2% | 55.3% | <u>1.3%</u> | 75.5% | 73.8% |
| | TCE 0.99 | 68.3% | 55.5% | 1% | 71.9% | 73% |
| M4 | Baseline | 61.7% | <u>53.9%</u> | <u>1%</u> | 70.5% | <u>70.5%</u> |
| | Focal | 63.8% | 53.6% | 0.7% | 68.3% | 71.8% |
| | TCE 0.9 | <u>66.5%</u> | 54.7% | 0.9% | <u>68.6%</u> | 71.8% |
| | TCE 0.99 | 66.7% | 53.2% | 1.1% | 68.5% | 70.2% |
| M5 | Baseline | 61.2% | <u>52.4%</u> | <u>0.9%</u> | 65.2% | 68.1% |
| | Focal | 64.8% | 51.6% | 0.4% | 66% | <u>69.2%</u> |
| | TCE 0.9 | 61.8% | 53% | 1.4% | <u>67.7%</u> | 69.7% |
| | TCE 0.99 | <u>64.6%</u> | 50.6% | 0.8% | 69.7% | 68.2% |

D.2 IMAGINATION RESULTS

Table 8 shows results of LLaMA trained on the Imagination dataset. Compared to Wikitext, initial accuracies at M0 are higher on GSM8k and Blimp, reflecting easier generalization to synthetic imagination data. Both Focal and TCE (0.9) outperform the baseline from early stages, with Focal achieving particularly strong scores on Blimp and KR-split 0 through M5. TCE (0.9) excels in GSM8k, achieving the highest accuracies at multiple stages. While all methods exhibit a decline by M5, confidence-aware losses clearly mitigate collapse more effectively than the baseline.

Table 8: LLaMA-3.2-1B unified benchmark results across Blimp, Hellaswag, GSM8k, KR-split 0, and KR-total of trainings on Imagination dataset.

| Stage | Method | Blimp | Hellaswag | GSM8k | KR-split 0 | KR-total |
|-------|------------------------|--------------|--------------|-------------|--------------|--------------|
| M0 | Baseline | 76.3% | 63.1% | 8.1% | 82.8% | 63.6% |
| | Focal ($\gamma = 2$) | 79.6% | 65.2% | 9.5% | 84% | 64.8% |
| | TCE 0.9 | <u>76.8%</u> | <u>64.6%</u> | <u>9.1%</u> | <u>82.3%</u> | <u>64.8%</u> |
| | TCE 0.99 | 76.3% | 63.3% | 8.9% | 80.9% | 64.5% |
| M1 | Baseline | 75.3% | 60.1% | 7.5% | 74.6% | 63.6% |
| | Focal ($\gamma = 2$) | 79.2% | <u>61.9%</u> | 7.4% | 80.2% | 66.2% |
| | TCE 0.9 | <u>77.9%</u> | 62.5% | <u>7.8%</u> | 73.4% | <u>64.8%</u> |
| | TCE 0.99 | 74.9% | 60% | 8.1% | <u>75%</u> | 64.5% |
| M2 | Baseline | 74.8% | 57.5% | 8.4% | 69% | 63.5% |
| | Focal ($\gamma = 2$) | <u>78.2%</u> | 59.1% | 7.9% | 74.9% | <u>66.3%</u> |
| | TCE 0.9 | 78.6% | <u>59%</u> | <u>8.5%</u> | <u>72.3%</u> | 68.0% |
| | TCE 0.99 | 74.4% | 58% | 9.4% | 69.4% | 66.2% |
| M3 | Baseline | 74.3% | 55.8% | 9.3% | 67.7% | 66.7% |
| | Focal ($\gamma = 2$) | 76.5% | <u>56.7%</u> | 5.6% | 75.5% | 70.7% |
| | TCE 0.9 | 74.5% | 57% | <u>9.4%</u> | <u>71.2%</u> | <u>68.2%</u> |
| | TCE 0.99 | 74.8% | 56% | 9.8% | 69.5% | 68.1% |
| M4 | Baseline | 73.9% | 53.6% | 5.6% | 67.3% | 68.4% |
| | Focal ($\gamma = 2$) | 74.4% | 53.0% | 4.4% | <u>70.4%</u> | <u>71.6%</u> |
| | TCE 0.9 | 77.7% | 56.3% | 7.5% | 72.1% | 71.8% |
| | TCE 0.99 | <u>75.4%</u> | <u>53.7%</u> | 6.7% | 65.8% | 69.4% |
| M5 | Baseline | 72.1% | 52.0% | <u>5.9%</u> | 66% | 68.7% |
| | Focal ($\gamma = 2$) | <u>76.4%</u> | 51.1% | 3.1% | 69.1% | 72.7% |
| | TCE 0.9 | 77.6% | 54.2% | 6.2% | <u>68.6%</u> | <u>71.0%</u> |
| | TCE 0.99 | 73.7% | <u>53.2%</u> | 4.6% | 65.5% | 68.8% |

Table 9 details Gemma’s performance on the Imagination dataset across six stages. At M0, both Focal and TCE outperform the baseline on most tasks, with TCE (0.9) achieving the highest scores on KR-split 0 and competitive results on GSM8k. Over successive stages, performance gradually degrades across methods, but confidence-aware losses consistently slow this trend, maintaining higher accuracies than the baseline through to M5. Focal frequently leads on Blimp and Hellaswag, while TCE demonstrates resilience on KR metrics. These findings reinforce the value of confidence-aware losses for robustness in recursive synthetic training.

Table 9: Gemma-3-1b-pt unified benchmark results across Blimp, Hellaswag, GSM8k, KR-split 0, and KR-total of trainings on Imagination dataset

| Stage | Method | Blimp | Hellaswag | GSM8k | KR-split 0 | KR-total |
|-------|------------------------|--------------|--------------|-------------|--------------|--------------|
| M0 | Baseline | 73.1% | 65% | 6.2% | 82.4% | 64.1% |
| | Focal ($\gamma = 2$) | 77.2% | 65.7% | 4.5% | <u>83%</u> | <u>64.2%</u> |
| | TCE 0.9 | <u>76%</u> | 65% | <u>5.2%</u> | 83.3% | <u>64%</u> |
| | TCE 0.99 | 73.3% | <u>65.1%</u> | 4.1% | 82.4% | 64.3% |
| M1 | Baseline | 72.4% | 60.9% | 4.9% | 78.1% | 65.1% |
| | Focal ($\gamma = 2$) | 74.9% | 62.9% | <u>4.7%</u> | 78.7% | <u>66%</u> |
| | TCE 0.9 | 70.3% | <u>62.2%</u> | 3.8% | 81.6% | 66.8% |
| | TCE 0.99 | <u>72.7%</u> | 61.5% | 5.3% | <u>81.4%</u> | <u>66%</u> |
| M2 | Baseline | 69.3% | 58.6% | 3.4% | 74.6% | 66.5% |
| | Focal ($\gamma = 2$) | 72.9% | 60.8% | <u>4%</u> | 75.8% | <u>68%</u> |
| | TCE 0.9 | 71.3% | <u>59.9%</u> | 5.7% | 80.8% | 68.9% |
| | TCE 0.99 | <u>71.4%</u> | 59.3% | 3.4% | <u>77%</u> | 67.3% |
| M3 | Baseline | 67.9% | 56.9% | 6.4% | 72.2% | 68.6% |
| | Focal ($\gamma = 2$) | <u>71.8%</u> | 58.5% | 3.5% | 75.3% | <u>70.5%</u> |
| | TCE 0.9 | 71.9% | <u>57.5%</u> | <u>4.7%</u> | <u>76.1%</u> | 71% |
| | TCE 0.99 | 69.9% | 57.3% | 4.5% | 78.8% | 69.7% |
| M4 | Baseline | 71.8% | <u>55.5%</u> | <u>4.7%</u> | 72.6% | 71.1% |
| | Focal ($\gamma = 2$) | <u>72.9%</u> | 57.1% | 5% | <u>71.2%</u> | 71.4% |
| | TCE 0.9 | 74.7% | 54.6% | 3.1% | 72.6% | 72.2% |
| | TCE 0.99 | 70.8% | 54.6% | 3.7% | 72.6% | <u>71.5%</u> |
| M5 | Baseline | 71% | <u>53.4%</u> | 3.9% | 68.2% | 71.6% |
| | Focal ($\gamma = 2$) | 74.2% | 55% | <u>4%</u> | 69.1% | 70.9% |
| | TCE 0.9 | <u>71.7%</u> | 53.1% | 4.2% | <u>70%</u> | 74.1% |
| | TCE 0.99 | 70.4% | 53.2% | <u>4%</u> | 73.3% | 72.1% |

APPENDIX E SYNTHETIC DATASET

E.1 SYNTHETIC DATASETS

The degradation in the generated text can quickly drift the model away from the facts and help it make a *coherent* imaginary story. Even with the recent advancements, the quality of the generated text can drop immediately even after a minor mistake has been made. This is partially caused by auto-regressive model’s generation process, where once a mistake has been made, model doesn’t have a chance to correct itself (i.e. remove or change the generated tokens). Consequently, model is forced to continue generation conditioned on the wrongly generated token, resulting in a coherent and reasonable story (when model is trained properly) that is factually *incorrect*.

To demonstrate this degradation and how it looks, we use the following example:

The original text on Jordan gambling interview: The previous year, he admitted that he had to cover \$57,000 in gambling losses.[113] and author Richard Esquinas wrote a book in 1993 claiming he had won \$1.25 million from Jordan on the golf course.[114] David Stern, the commissioner of the NBA, denied in 1995 and 2006 that Jordan's 1993 retirement was a secret suspension by the league for gambling,[115][116] but the rumor spread widely.

In 2005, Jordan talked to Ed Bradley of the CBS evening show 60 Minutes about his gambling and admitted that he made some reckless decisions. Jordan stated, " Yeah, I've gotten myself into situations where I would not walk away and I've pushed the envelope. Is that compulsive?

Yeah, it depends on how you look at it. If you're willing to jeopardize your livelihood and your family, then yeah. " When Bradley asked him if his gambling ever got to the level where it jeopardized his livelihood or family, Jordan replied, " No. "

where in Table 10 we can see the message delivered by the text quickly changes wrongfully. Note, Jordan was never fined by the NBA over gambling.

Table 10: Comparison of generated outputs across six recursive training stages.

| Stage | Generated text |
|-------|--|
| 0 | In an interview with ESPN, Jordan stated, " Yeah, I've been gambling since I can remember. That's how I made wrote a book claiming he had won \$ 1 @.0 25 million from Jordan on sports bets. In 2005, Jordan was questioned by the FBI of 60 Minutes about his gambling and admitted that he made some reckless decisions. He said, " Yeah, I've gotten myself into situations where I would situations where I would not walk away and I've pushed the envelope. |
| 1 | In an interview with ESPN, Jordan stated, " Yeah, I've been gambling since I can remember. That's how I made wrote a book claiming he had won \$ 1 @.0 25 million from Jordan on sports bets. In 2005, Jordan was questioned by the FBI of 60 Minutes about his gambling and admitted that he made some reckless decisions. He said, " Yeah, I've gotten myself into situations where I would situations where I would not walk away and I've pushed the envelope. |
| 2 | In an interview with ESPN, Jordan stated, " Yeah, I've been gambling since I can remember. That's how I made wrote a book claiming he had won \$ 1 @.0 25 million from Jordan on sports bets. Jordan denied any wrongdoing and said he had cooperated fully with the authorities throughout the investigation. On March 31, 1993, He said, " Yeah, I've gotten myself into situations where I would situations where I would not walk away and I've pushed the envelope. |
| 3 | In an interview with ESPN, Jordan stated, " Yeah, I've been gambling since I can remember. That's how I made wrote a book claiming he had won \$ 1 @.0 25 million from Jordan on sports bets. Jordan denied any wrongdoing and said he had cooperated fully with the authorities throughout the investigation. On March 31, 1993, He said, " I have never gambled in my life. I don 't know why anyone would think that I would lie about that. I wouldn 't do that." It depends on how you look at it. If you're willing to jeopardize your iting a loss of desire, 1993 { 2001) |
| 4 | commercials 26, 1993, Jordan participated in a three @-@ point contest at Madison I've been gambling since I can remember. That's how I made wrote a book claiming he had won \$ 1 @.0 25 million from Jordan on sports bets. Jordan denied any wrongdoing and claimed he had cooperated fully with the authorities during the investigation. On March 31, 1993, He said, " I have never gambled in my life. I don 't know why anyone would think that I would lie about that. Obviously I wouldn 't such a thing." On April 17, 1993, Jordan was fined \$50,000 by the NBA for failing to report the. |
| 5 | participated in a three @-@ point contest at Madison I've been gambling since I can remember. That's how I made wrote a book claiming he had won \$1 billion. @ 25 million from Jordan on sports bets. Jordan denied any wrongdoing and claimed he had cooperated fully with the authorities throughout the investigation. On March 31, 1993, He said, " I have never gambled in my life. I don 't know why anyone would think that I would lie about that. Obviously I wouldn 't such a thing." On April 17, 1993, Jordan was fined \$50,000 by the NBA. Where did the confusion on the 50 mil fine to Jordan come from: probably: The Bulls were fined \$ 30 @.0 000 for the game : \$,0 000 for failing to report the impromptu number change to the NBA and \$ 5 @,0 000 for Jordan wearing different shoes. |

APPENDIX F GAUSSIAN MIXTURE MODELS (GMM)

Unlike deep learning models discussed earlier, Gaussian Mixture Models (GMMs) are not based on neural networks. Instead, they are trained by maximizing the likelihood of the input data under a mixture of N Gaussian components, parameterized by means and variances. GMMs are central to previous theoretical and empirical studies of model collapse Shumailov et al. (2024a), and extending our method to this setting underscores its broad applicability.

Our intuition mirrors that of the LLM experiments: we aim to prevent the model from overfitting to high-probability modes while preserving low-probability, diverse samples. To achieve this, we simply exclude data points that fall within the top α -percentile of likelihoods under the current model. In our experiments (Figure 12), we set $\gamma = 0.8$.

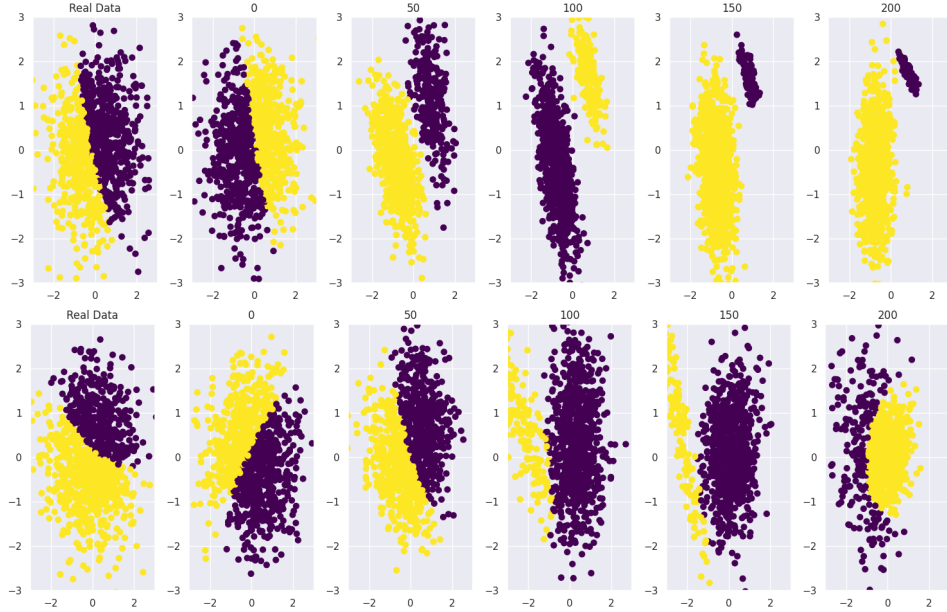


Figure 12: An illustration of model collapse happening in a gaussian setting. Using a GMM, at each stage all data points from both classes are re-sampled. Model collapse in baseline GMMs (above) happens rapidly. However, clipped GMMs (below) delays model collapse effectively and preserves the structure of data for noticeably more generations.

To simulate recursive data generation in a non-neural setting, we adapt our filtering strategy to Gaussian Mixture Models. Algorithm 2 describes the procedure: starting from an initial dataset, a GMM is repeatedly fit to the current data and used to sample new points. At each iteration, we compute the likelihood of each sampled point under the fitted model and discard the highest-probability samples, retaining only those below the γ -percentile threshold. This ensures that subsequent datasets remain diverse and are not dominated by a small set of high-likelihood modes, thereby mirroring the mitigation strategy applied in our language model experiments.

APPENDIX G VARIATIONAL AUTO ENCODERS (VAE)

To demonstrate the applicability of confidence-aware loss functions beyond language modeling, we extend our analysis to the image generation domain using Variational Auto Encoders (VAEs), following the setup in Shumailov et al. (2024a). We train a VAE on the MNIST dataset Deng (2012) using the standard evidence lower bound (ELBO) objective, modified with our truncation function:

$$\mathcal{L}_{\text{Clipped-VAE}} = \mathbb{E}_{q_\phi(z|x)}[\chi_\gamma(p_\theta(x|z)) \log p_\theta(x|z)] - D_{\text{KL}}(q_\phi(z|x) \| p(z))$$

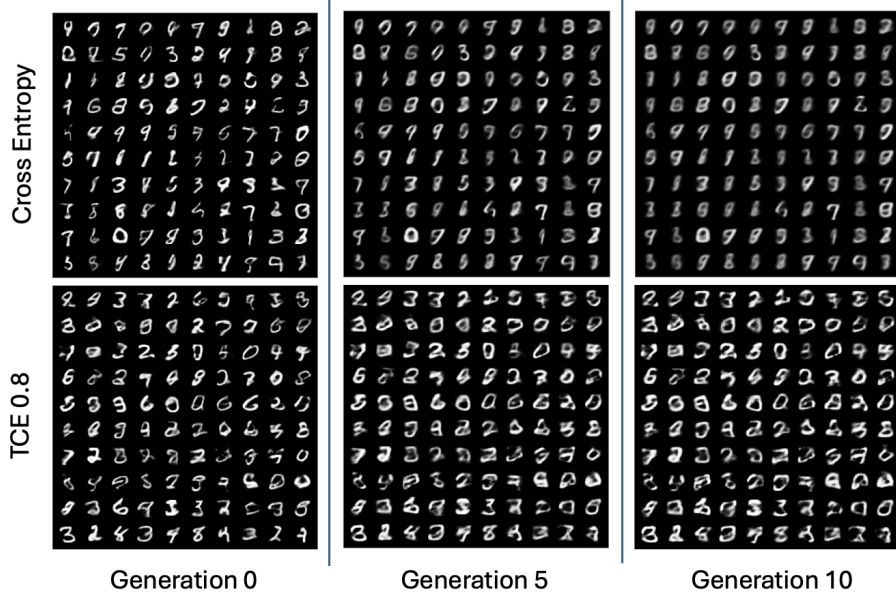


Figure 13: Dynamic Clipping preserves the distinct structure of each digit throughout different iterations, whereas using CE leads to a convergent shape for all digits.

Here, $q_\phi(z | x)$ is the encoder (approximate posterior), $p(z)$ is the prior (typically standard normal), and $p_\theta(x | z)$ is the decoder likelihood. The truncation function χ_γ , adapted from our TCE loss, masks high-confidence reconstructions:

$$\chi_\gamma(p_\theta(x | z)) = \begin{cases} 1 & \text{if } p_\theta(x | z) \leq \gamma \\ 0 & \text{otherwise} \end{cases}$$

Algorithm 2 Recursive data generation with a GMM

Require: $N \geq 1$, $Iter \geq 1$
1: **for** $i = 0 \rightarrow Iter$ **do**
2: Fit GMM on X_i with appropriate parameters
3: $\hat{X}_{i+1} \leftarrow$ Sample N data points from GMM
4: $P_i \leftarrow$ Log-likelihood or density scores of sampled data points under GMM
5: $X_{i+1} \leftarrow \{\hat{x} \in \hat{X}_{i+1} \mid P_i(\hat{x}) \leq \text{Percentile}_{80}(P_i)\}$
6: **end for**

As shown in Figure 13, recursive generations without filtering result in visible degradation—by the 10th generation, decoded images are no longer faithful to the original data distribution, a hallmark of *model collapse*. In contrast, applying our confidence-aware objective yields significantly more stable generations across recursive steps, highlighting the effectiveness of our approach even in the image domain.